

# Graph Attention Reinforcement Learning for Age-Optimal Multicast Scheduling and Routing

Yanning Zhang, *Member, IEEE*, Guocheng Liao, *Member, IEEE*, Shengbin Cao,  
Ning Yang, *Member, IEEE*, Nikolaos Pappas, *Senior Member, IEEE*, and Meng Zhang, *Member, IEEE*

**Abstract**—*Age of Information (AoI)* has emerged as a prominent metric for evaluating the timeliness of information in time-critical applications. Applications, including video streaming, virtual reality, and metaverse platforms, necessitate the use of multicast communication. Optimizing AoI in multicast networks is challenging due to the coupled multicast routing and scheduling decisions, the network dynamics, and the complexity of the multicast. This paper focuses on dynamic multicast networks and aims to minimize the expected average AoI through the integration of multicast routing and scheduling. To address the inherent complexity of the problem, we first propose to apply reinforcement learning (RL) to learn the heuristics of multicast routing, based on which we decompose the original problem into two subtasks that are amenable to hierarchical RL methods. Subsequently, we propose an innovative framework based on graph attention networks (GATs) and prove its contraction mapping property. Such a GAT framework effectively captures graph information used in the hierarchical RL framework with superior generalization capabilities. To validate our framework, we conduct experiments on three datasets, including a real-world dataset called AS-733, and show that our proposed scheme reduces the average weighted AoI by 38.2% and the weighted peak age by 43.4% compared to baselines over all datasets in dynamic networks.

**Index Terms**—Age of Information, Multicast, Routing, Cross-layer Design, Reinforcement Learning, Graph Embedding Methods.

## I. INTRODUCTION

### A. Background and Motivations

**R**EAL-time applications in various domains, such as human-computer interaction [1], monitoring systems [2] and Internet-of-Things (IoT) [3] have gained significant attention recently. These applications require timely updates to ensure accurate and timely information availability for critical tasks like decision-making, user interaction, and system control [4]. While delay is a commonly used metric in communication networks [5], it is now recognized that ensuring timely updates is distinct from simply minimizing delay [6].

Yanning Zhang and Meng Zhang are with the Zhejiang University - University of Illinois Urbana-Champaign Institute, Zhejiang University (E-mail: yanning.22@intl.zju.edu.cn, mengzhang@intl.zju.edu.cn).

Guocheng Liao is with Sun Yat-Sen University (E-mail: liaogch6@mail.sysu.edu.cn).

Ning Yang is with the Institute of Automation, Chinese Academy of Sciences (E-mail: ning.yang@ia.ac.cn).

Nikolaos Pappas is with the Department of Computer and Information Science (IDA), Linköping University (E-mail: nikolaos.pappas@liu.se).

For instance, although maximizing the speed of sensor updates may optimize utilization, it can result in delayed statuses being received by the monitor due to a backlog of status messages in the system. Consequently, there is a need for a metric that captures the timeliness of information dissemination. The concept of *Age of Information (AoI)* has emerged as a promising metric in various domains, including learning and network protocols [7]. AoI quantifies the freshness of information that a monitor possesses about a specific entity or process, which has been identified as a suitable metric for evaluating the system performance [8], making it particularly relevant for real-time applications [9].

Multicast plays a crucial role in the networking of numerous trending real-time applications, making it an essential communication paradigm. For the Internet to scale effectively, multicast is not merely an option but an imperative requirement [5]. Real-time multicast applications, such as video streaming [10] and intelligent transportation systems [11], have experienced significant growth in recent times. One of the primary problems lies in the routing process, which entails determining the optimal paths from the source to destinations [5]. Multicast routing problems fall within the domain of Combinatorial Optimization (CO) problems and are NP-hard [12], which are computationally infeasible to solve in large-scale networks. Researchers have proposed approximation algorithms for this category of problems (e.g., [13], [14]).

To deal with the complexity of multicast problems, researchers have proposed various approximation algorithms to optimize the multicast process [15]. However, due to the inherently distributed feature of network systems, a traditional controller can only optimize the routing process with local information. Fortunately, recent advances in Software-defined Networking (SDN) have enabled the intelligent control of network devices [16]. SDN is a network architecture that separates the control plane from the data plane, where the control plane is centralized and is responsible for managing network resources and programming the network dynamically. The centralized controller has a global network view by monitoring and collecting the real-time network state (e.g., packets) and configurations. The above features ensure that the solutions provided by intelligent algorithms (e.g., AI-based algorithms) can be implemented in real-world scenarios.

On the other hand, compared to minimizing the delay or cost in a static network, AoI scheduling prevents backlogs

of updates or additional resource depletion, which is crucial in real-time applications (e.g., [17], [18]). Some studies have considered *multicast scheduling* problems in optimizing AoI (e.g., [8]). However, they tend to overlook the multicast routing problem. This is related to the black box approaches in traditional TCP/IP networks, which prevent necessary information sharing between layers [19]. Cross-layer design methods have been proposed to mitigate these side effects. Usually, cross-layer design methods attempt to go beyond black box approaches. It has been shown that cross-layer design can improve network performance by jointly optimizing routing and scheduling decisions (e.g., [20], [21]). Therefore, a cross-layer multicast framework is suitable for optimizing AoI by joint multicast routing and scheduling decisions.

Furthermore, real-world networks often operate under energy constraints, where the overall energy consumption of the network is limited [22]. This introduces additional complexity to the problem because a trade-off exists between energy consumption and AoI [23], making the existing multicast algorithms inapplicable. It is worth noting that the energy consumption of a multicast network is closely related to multicast scheduling decisions. For instance, a multicast tree with more destinations may lead to lower AoI but higher energy consumption. Hence, there is a clear demand for a novel multicast scheme that offers a comprehensive solution for optimizing AoI in energy-constrained multicast networks.

In this paper, we aim to answer the following main question: *How should one design multicast scheduling and routing algorithms to minimize the age of information?*

### B. Key Challenges and Solution Approach

We now summarize the key challenges of answering the above question as follows:

- 1) **Cross-Layer Design.** Multicast scheduling and routing are intertwined, both having an impact on the AoI of destinations. However, existing methods often treat them separately, leading to a suboptimal solution. The high-dimensional nature of the problem also makes it difficult to solve the joint problem directly. Therefore, designing a cross-layer framework that can jointly optimize multicast scheduling and routing decisions is essential.
- 2) **Unknown System Dynamics.** Real networks often exhibit dynamic behavior, and the statistical properties of these network dynamics are difficult to obtain. Traditional multicast algorithms often rely on static routing tables or predefined distributions that are unsuitable for dynamic scenarios.
- 3) **Time-varying Optimal Solutions.** Optimizing AoI in multicast networks requires making decisions at each time slot, which requires time-varying optimal solutions. Existing methods often fail to capture the time-varying nature of the problem and need to be re-optimized repeatedly, which is computationally infeasible.

First, solving multicast problems requires addressing them on a case-by-case basis, as solutions can vary based on the

representation of the underlying graph data. This is particularly true in real-time multicast applications, in which different subsets of users are scheduled for multicast communication in each time slot. To tackle this challenge, we propose the use of a tree-generating heuristic algorithm inspired by the work of [24]. The fundamental concept is to incrementally add nodes and edges to a graph structure while satisfying the tree constraint. Previous research [24] has demonstrated that employing a greedy meta-algorithm within a Reinforcement Learning (RL) framework yields solutions that closely approach optimality in many combinatorial optimization problems. Second, to jointly solve the age-optimal multicast scheduling and routing problem, we first decompose the original problem into two subproblems: the scheduling subproblem and the tree-generating subproblem. This decomposition lowers the complexity of the original problem and makes it amenable to a cross-layer design.

As described in challenge 2, the unknown system dynamics make it difficult to obtain the optimal solutions. Specifically, most existing methods can only provide solutions for a specific network scenario. When the network topology changes, the solutions are no longer applicable. Furthermore, Challenge 3 is crucial for optimizing AoI in multicast networks, even if the network topology is fixed. This is because the AoI of destinations is determined not only by the solutions at a specific time but also by multiple previous decisions. For instance, previously generated packets may arrive at the destinations at different times, leading to different AoI values. To address this challenge, we reformulate the scheduling and tree-generating subproblems into Markov Decision Processes (MDPs) and learn policies that can adapt to unknown system dynamics. Considering the relation between two MDPs, we propose a hierarchical Reinforcement Learning (RL) framework that can be generalized to unseen networks without retraining.

One remaining problem is the optimization of the above policies. The non-Euclidean nature of graphs leads to the high-dimensional state space and action space of MDPs, making RL methods inefficient when exploring the state-action space. Therefore, the following additional challenge arises:

- 4) **High-dimensional Graph Information.** Traditional methods are inefficient when extracting relevant graph features due to the non-Euclidean nature of graphs, even in machine learning methods. The hidden graph information is crucial for making decisions in multicast networks.

To address the above challenge, an effective graph embedding method is required to extract hidden graph information while reducing the dimensionality. An existing work utilized graph embedding methods and reinforcement learning to learn a heuristic quality function for CO problems, which has shown promising results [24]. We extend this method to multicast networks. First, we consider one type of Graph Neural Network [25], Graph Attention Networks (GATs) [26], which is a graph embedding method that has shown superior performance in capturing graph information. Then, we develop a quality

function to measure the performance of multicast trees, which is used to learn routing decisions in the hierarchical RL framework. In addition, the contraction mapping property of existing GATs is not well understood, which is crucial for the convergence of our model. To address this issue, we propose a novel type of GAT as a contraction mapping property. A convergence analysis is also provided.

We summarize our main contributions as follows:

- **Joint Multicast Scheduling and Routing Problem:** We formulate the first problem of joint multicast routing and scheduling, accounting for energy constraints and potential network dynamics. *This is the first work to consider the problem of joint multicast scheduling and routing for minimizing AoI to the best of our knowledge.*
- **Hierarchical RL Framework.** To address challenges 1, 2, and 4, we first propose to apply reinforcement learning (RL) to learn the heuristics of multicast routing, based on which we decompose the problem into two subtasks, which can be naturally captured by a hierarchical RL framework. The primary subtask involves selecting destinations over time, while the invoked subtask generates multicast trees.
- **A Variant of Graph Attention Network.** To reduce the curse of dimensionality of the decision-making within the RL framework, we introduce a novel variant of the Graph Attention Network (GAT) that leverages the attention mechanism to extract graph information. Our proposed GAT achieves a provable convergence guarantee through its contraction mapping property.
- **Experimental Results.** We validate our approach using three datasets, which include the AS-733 real-world dataset. TGMS outperforms other baselines (non-cross-layer design, existing multicast algorithms, and methods without graph embedding). It can achieve an average reduction in AoI of 38.2% while satisfying the energy consumption constraint.

## II. RELATED WORKS

### A. Multicast Routing

*Multicast routing* poses a significant challenge in various scenarios, including ad hoc networks [27] and Internet of Things (IoTs) systems [28]. It has also gained research interest in cooperative games [29]. A substantial body of research has focused on optimizing multicast routing in various scenarios. Due to the distribution of network entities, a spanning tree has been considered one of the most efficient and viable mechanisms for multicast routing [15]. Considering various requirements, different types of trees have been proposed, with the Steiner tree being one of the most popular types [30]. Given a set of terminal nodes, a Steiner Tree Problem (STP) finds a tree that connects all terminal nodes at the minimum cost. The STP falls within the domain of CO problems which are proved to be NP-hard [12]. Researchers have proposed various algorithms to solve the STP. For instance, Byrka *et al.*

[13] developed an LP-based approximation algorithm to solve the STP with a 1.55 approximation ratio. Fischetti *et al.* [14] reformulates the STP as a mixed-integer linear programming problem and proposes a linear time algorithm to solve it, while the edge costs are assumed to be the same. *However, the same optimization problem needs to be re-optimized at each time slot for the above methods due to the time-varying nature of networks, which is computationally infeasible.*

### B. Age of Information

The concept of *AoI* was initially introduced by Kaul *et al.* [6] and garnered significant attention in wireless scenarios (e.g., [31], [32], [33], [34]) and queue theory (e.g., [35], [36], [37]). In the context of multicast networks, a substantial body of research has primarily concentrated on analyzing stopping schemes to optimize AoI. For instance, Li *et al.* [8] considered fixed and randomly distributed deadlines for multicast status updates in a real-time IoT system. Buyukates *et al.* [38] considered a multi-hop multicast network and determined an optimal stopping rule for each hop for exponential link delays. *Despite the success of these works in reducing AoI, the considered problem settings are relatively simple for real scenarios.* Some studies focus on serving policies to optimize multicast AoI. For example, Bedewy *et al.* [39] prove that a preemptive last-generated, first-served policy results in smaller age processes than other causal policies. *However, the energy consumption is not considered in their work.*

On the other hand, to deal with the complexities of real-world scenarios, researchers have delved into leveraging *Machine Learning Methods* to optimize AoI in diverse fields, including UAV-assisted systems (e.g., [40], [41], [42], [43]), IoTs systems (e.g., [44]) and intelligent transportation systems (e.g., [45]). This line of work mainly focuses on optimal resource allocation and trajectory design to achieve AoI optimization. Part of the research considered scheduling policies for optimizing AoI. For instance, Zhang *et al.* in [46] reformulated a scheduling problem as a Markov game to optimize the AoI of industrial applications. He *et al.* in [47] proposed a Deep RL-based scheduling algorithm for real-time applications in mobile edge computing systems. *Although these works have achieved promising results, they did not consider the graph information in multicast networks, making them inapplicable to multicast scenarios.*

Furthermore, AoI has also gained research interest in energy harvesting networks, especially in IoT scenarios (e.g., [48], [49], [50]). Deep RL methods are also applied to optimize the trade-off between AoI and energy consumption (e.g., [51]). Some studies have considered this trade-off for multicast networks. For instance, Xie *et al.* [23] considered different stopping schemes for multicast networks to maximize energy efficiency while minimizing AoI. Nath *et al.* [52] considered a similar problem and proposed an optimal scheduling strategy. *However, these approaches did not account for the relation between multicast routing and scheduling.*

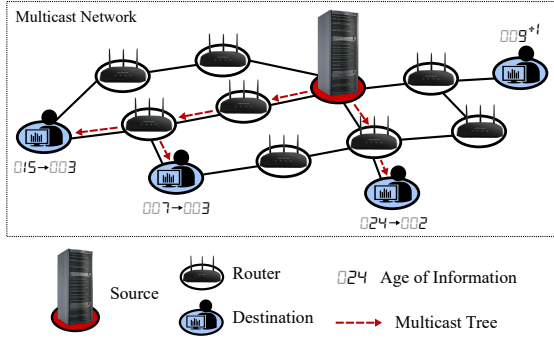


Fig. 1. An example of a multicast network. The nodes are connected by links with different costs. At the beginning of each time slot, the source generates update packets, which are then forwarded to a part of the destinations by routers. The packets traveling through different paths may not arrive at the destinations simultaneously, making the AoI of destinations different.

### III. SYSTEM MODEL

#### A. System Overview

We consider a multicast network, as illustrated in Fig. 1. The system operates for an infinite horizon of discrete slotted time  $t \in \mathbb{N}$ , where  $\mathbb{N}$  is the set of all natural numbers. We characterize the network topology by a dynamic (undirected) graph, and the graph at time  $t$  is denoted as  $\mathcal{G}_t = \{\mathcal{V}_t, \mathcal{E}_t\}$ , where  $\mathcal{V}_t$  represents the set of nodes and  $\mathcal{E}_t$  represents the set of undirected links. There are three distinct categories of nodes in each  $\mathcal{V}_t$ :

- **The Source Node.** The network includes a designated source node that generates updates for a multicast group, e.g., a video streaming server. Assume that the source node can generate at least one update packet for each destination at each time slot.
- **Router Nodes.** Router nodes are responsible for forwarding update packets to destinations. The forwarding process is based on multicast routing decisions.
- **Destination Nodes.** Destination nodes are expected to receive status updates continuously from the source node, e.g., subscribers in a video streaming service. The set of destinations at time  $t$  is denoted as  $\mathcal{U}_t \subset \mathcal{V}_t$ .

**Remark 1.** Multicast communication can be classified into two types: source-specific multicast and group-shared multicast [53]. The above network setting can also be applied to group-shared multicast, where the source node is the node that sends data to other destinations at time  $t$ . When multiple sources transmit simultaneously, we consider the transmitting process for each of them independently.

This setting applies to various scenarios. For example, consider a virtual reality experiment in which users are attending a live performance. Another example is the intelligent transportation system, where a traffic management center multicasts real-time traffic updates to multiple vehicles or roadside units.

**Network Dynamics.** Real-world networks often exhibit *dynamic behaviors*. For instance, in wireless networks, topology

changes due to node mobility or link instability. We assume that the network topology  $\mathcal{G}_t$  follows a stochastic process. This assumption has been widely adopted (e.g., [54]). We first define the link indicator  $\sigma(e, t)$  as follows:

$$\sigma(e, t) = \begin{cases} 1, & \text{if link } e \in \mathcal{E}_t, \\ 0, & \text{otherwise.} \end{cases} \quad (1)$$

For a network with a set of nodes  $\mathcal{V}_t$ , the set of links at time  $t$  is denoted as  $\xi(t) = \{\sigma(e, t) | e \in \mathbb{R}^{|\mathcal{V}_t| \times |\mathcal{V}_t|}\}$ . Let  $\Xi$  denote all possible network topologies. For any time slot  $t$ ,  $\xi(t)$  evolves as follows:

$$\sum_{\xi(t) \in \Xi} p(\xi(t)) = 1, p(\xi(t)) > 0, \forall \xi(t) \in \Xi. \quad (2)$$

The statistical property of (2) depends on specific network scenarios, which is assumed unknown a priori.

#### B. Multicast Process

Here, we describe the *multicast process* in the network. At the beginning of each time slot, the source node generates multiple update packets, which will be transmitted between router nodes, and eventually arrive at the destination nodes. We assume that the source can generate packets at will, where each packet includes an address of its destination. We consider the following rule of delay:

**Assumption 1.** The delay between the source and the destination is linearly proportional to the hops between them.

**Remark 2.** The above assumption has been proven to be valid in many multi-hop scenarios (e.g., [55], [56], [57]). When it is not satisfied, the extension to a more general cast is conceptually straightforward by using the sum of delays between nodes instead of hops. This does not alter our main results.

Under the above paradigm, we can normalize the one-hop delay for a packet as a single time slot. For the network layer, We consider an error-free transmission (e.g., [58]) with an adaptive power scheme to compensate for potential deep fading scenarios (e.g., [59]). Hence, a packet can be transmitted from node  $i$  to node  $j$  if the link  $(i, j)$  exists in  $\mathcal{E}_t$ , which takes one time slot with an average energy cost of  $C_{i,j}$ . If multiple packets arrive at a destination node simultaneously, only the packet with the smallest AoI is considered.

Next, we describe the *multicast scheduling decisions*. At the start of time slot  $t$ , a controller can select a subset of destination nodes  $\mathcal{U}'_t \subseteq \mathcal{U}_t$  to generate updates for (the updates may not received immediately), which we refer to as multicast scheduling in this paper. It is crucial to trade off energy consumption and AoI reduction.

Now we define the *multicast routing decisions*. Due to the one-source-multiple-destination nature of multicast problems, multicast trees are widely used to represent multicast routing

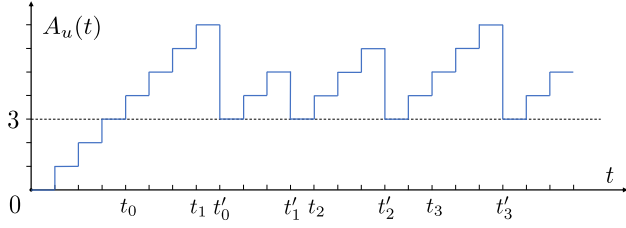


Fig. 2. An example of the AoI. Time  $t_k$  denotes the time when the  $k$ -th packet is generated while  $t'_k$  denotes the time when it arrives. The AoI of destination  $u$  is updated upon the reception of a packet update and based on the age of the packet (3 in this case) at time  $t'_k$ .

decisions [12]. Let  $\mathcal{T}_t$  denotes a multicast tree at time slot  $t$  of  $\mathcal{G}_t = \{\mathcal{V}_t, \mathcal{E}_t\}$ , i.e.:

$$\mathcal{T}_t = \{\mathcal{V}_t^{\mathcal{T}}, \mathcal{E}_t^{\mathcal{T}}\}, \mathcal{V}_t^{\mathcal{T}} \subseteq \mathcal{V}_t, \mathcal{E}_t^{\mathcal{T}} \subseteq \mathcal{E}_t. \quad (3)$$

The multicast tree  $\mathcal{T}_t$  has two properties: (i) It is a connected acyclic undirected graph. (ii) The source node and the selected destinations  $\mathcal{U}_t^{\mathcal{T}}$  are included. The multicast routing process can be described as follows: at time slot  $t$ , the source generates  $|\mathcal{U}_t^{\mathcal{T}}|$  packets, which will be transmitted to their destinations along the multicast tree  $\mathcal{T}_t$  in the following time slots.

Due to possibly different hops from the source to different destinations in  $\mathcal{T}_t$ , the arrival times of packets generated at time  $t$  may be different (see Fig. 1). When a new multicast tree is generated, we let the previously generated packets stick to the plan, i.e., following the multicast tree at its generation. In a dynamic network, a link may be deactivated before packets arrive. In this situation, the packet will be dropped when it reaches the inactive link. We consider that the time scale of network topology changes is much larger than that of a packet transmission.

### C. Age-directed Multicast

To analyze the AoI of destinations, we define the *age of packet*. Let  $p \in \mathbb{N}$  denote a packet, the age of packet  $p$  is defined as:

$$\hat{A}_p(t) = t - t_p, \forall t \geq t_p, \quad (4)$$

where  $t_p \in \mathbb{N}$  denotes the time when packet  $p$  is generated and  $\hat{A}_p(t)$  increases linearly in time. The AoI of destination  $u \in \mathcal{U}_t$  is defined as:

$$A_u(t) = \begin{cases} \hat{A}_p(t), & \text{if } d_{u,p}(t) = 1, \\ A_u(t-1) + 1, & \text{otherwise,} \end{cases} \quad (5)$$

where  $d_{u,p}(t)$  is an indicator representing whether packet  $p$  arrives at destination  $u$  at time  $t$ . If packet  $p$  arrives at destination  $u$  at time  $t$ ,  $d_{u,p}(t) = 1$ ; otherwise,  $d_{u,p}(t) = 0$ . As shown in Fig. 2, if a destination  $u$  receives a packet at time  $t$ ,  $A_u(t)$  is updated to be the AoI of the received packet at that time. Otherwise,  $A_u(t)$  grows linearly with time. The average weighted AoI of the network is defined as:

$$\bar{A} \triangleq \limsup_{T \rightarrow \infty} \frac{1}{T} \sum_{t=0}^T \sum_{u \in \mathcal{U}_t} \omega_u A_u(t), \quad (6)$$

where  $\omega_u \in (0, 1)$  represents the weighted importance of a destination  $u \in \mathcal{U}_t$ .

To establish the relation between the AoI and multicast trees, we refer to the following lemma:

**Lemma 1** ([60]). Any two vertices in a tree can be connected by a unique simple path.

Considering the multicast process described above, we derive that the time required for a packet to reach destination  $u$  is equal to the number of hops between the source and destination  $u$  in a multicast tree  $\mathcal{T}_t$ , denoted as  $h_{\mathcal{T}_t}(u)$ . Then (5) can be rewritten as:

$$A_u(t + h_{\mathcal{T}_t}(u)) = \begin{cases} h_{\mathcal{T}_t}(u), & \text{if } u \in \mathcal{V}_t^{\mathcal{T}}, \\ A_u(t + h_{\mathcal{T}_t}(u) - 1) + 1, & \text{otherwise.} \end{cases} \quad (7)$$

That is,  $A_u(t + h_{\mathcal{T}_t}(u))$  will drop to  $h_{\mathcal{T}_t}(u)$  when a packet generated at  $t$  arrives at destination  $u$  at time  $t + h_{\mathcal{T}_t}(u)$ . Note that  $A_u(t)$  depends on two factors: (i) the generation intervals of packets for destination  $u$ ; (ii) the age of packets upon arrival, i.e.,  $h_{\mathcal{T}_t}(u)$ . Both factors are determined by multicast trees. Therefore, obtaining proper multicast trees is essential for optimizing AoI.

### D. Energy Consumption

Here we consider the *energy consumption* in multicast processes. The energy consumption of a multicast tree  $\mathcal{T}_t = \{\mathcal{V}_t^{\mathcal{T}}, \mathcal{E}_t^{\mathcal{T}}\}$  is defined as:

$$C(\mathcal{T}_t) \triangleq \sum_{(i,j) \in \mathcal{E}_t^{\mathcal{T}}} C_{i,j}. \quad (8)$$

This means that if we multicast packets from the source to the selected destinations  $\mathcal{U}_t^{\mathcal{T}}$  through the multicast tree  $\mathcal{T}_t$ , the total energy consumption is the sum of the energy costs of all links in  $\mathcal{T}_t$ . The energy consumption of a network is constrained by a long-term energy budget  $\bar{C}$ , which is represented as follows:

$$\lim_{T \rightarrow \infty} \frac{1}{T} \sum_{t=0}^T C(\mathcal{T}_t) \leq \bar{C}. \quad (9)$$

The presence of an energy consumption constraint will lead to a trade-off between energy consumption and AoI, which is a crucial consideration in multicast networks [23]. A multicast tree with more destinations may lead to lower AoI but higher energy consumption. Therefore, it is necessary to carefully select the destinations included in the multicast tree during each time slot, underscoring the significance of multicast scheduling.

### E. Age-minimal Multicast Scheduling and Routing

We now formally define the problem of age-minimal multicast scheduling and routing. Let  $\pi \triangleq \{\mathcal{T}_0, \mathcal{T}_1, \dots, \mathcal{T}_T\}$  denotes an update policy. We consider *causal policies*, in which control decisions are made based on the history and current

information of the network. Specifically,  $\mathcal{T}_t$  is determined based on  $\{\mathcal{G}_k, \mathcal{T}_k, A_u(k) | 0 \leq k \leq t-1, u \in \mathcal{U}_k\}$ . Our goal is to find a policy  $\pi$  to minimize the expected time-average AoI while satisfying the energy constraint. This problem can be formulated as follows:

$$\mathbf{OP:} \quad \min_{\pi} \limsup_{T \rightarrow \infty} \frac{1}{T} \mathbb{E}_{\pi} \left[ \sum_{t=0}^T \sum_{u \in \mathcal{U}_t} \omega_u A_u(t) \right], \quad (10a)$$

$$\text{s.t.} \quad \lim_{T \rightarrow \infty} \frac{1}{T} \mathbb{E}_{\pi} \left[ \sum_{t=0}^T C(\mathcal{T}_t) \right] \leq \bar{C}. \quad (10b)$$

The dual problem can be formulated as:

$$\mathbf{DP:} \quad \max_{\lambda \geq 0} \inf_{\pi} \lim_{T \rightarrow \infty} \frac{1}{T} \mathbb{E}_{\pi} \left[ \sum_{t=0}^T \sum_{u \in \mathcal{U}_t} \omega_u A_u(t) + \lambda \left( \sum_{t=0}^T C(\mathcal{T}_t) - T\bar{C} \right) \right], \quad (11)$$

where  $\lambda$  is the Lagrangian multiplier corresponding to (10b). The aforementioned problem encounters several challenges: (i) Policy  $\pi$  couples the multicast scheduling and routing decisions; (ii) the solution space of multicast trees is exponential in the number of destinations, making it computationally infeasible to solve the problem directly; (iii) the network dynamics are unknown, making it difficult to obtain the optimal solutions. Therefore, we reformulate the problem into subproblems and solve them sequentially, corresponding to the cross-layer design.

#### IV. PROBLEM REFORMULATION

Our main approach is to decompose the problem **DP** in (11) into a scheduling subproblem and a tree-generating subproblem. The scheduling subproblem is a primary problem that focuses on determining the destinations that need to be updated in each time slot, typically at a higher layer such as the transport layer. The tree-generating subproblem aims to obtain an optimal multicast tree for the chosen destinations, typically operating at a lower layer such as the network layer. The Lagrangian multiplier  $\lambda$  acts as a signal between the two layers.

##### A. Problem Decomposition

The two subproblems are formulated as follows:

**Definition 1 (Scheduling Subproblem).** Given a network  $\mathcal{G}_t$ , find a deterministic causal policy  $\pi_s = \{\mathcal{U}'_0, \mathcal{U}'_1, \dots, \mathcal{U}'_T\}$  of destination sets  $\mathcal{U}'_t \in \mathcal{U}_t$  to solve:

$$\mathbf{P1:} \quad \max_{\lambda \geq 0} \inf_{\pi_s} \lim_{T \rightarrow \infty} \frac{1}{T} \mathbb{E}_{\mathcal{U}'_t \sim \pi_s} \left[ \sum_{t=0}^T g(\lambda, \mathcal{U}'_t) \right], \quad (12)$$

where  $g(\lambda, \mathcal{U}'_t)$  is defined by the following tree-generating subproblem:

TABLE I  
NODE FEATURES ( $\mathbf{x}_t$ )

Features	Dim. per node
One-hot encoding of node type	3
Weighted node importance ( $\omega_u$ )	1
AoI of the node ( $A_u(t)$ )	1
Number of transmitting packets	1

**Definition 2 (Tree-generating Subproblem).** Given a network  $\mathcal{G}_t$  and a set of destinations  $\mathcal{U}'_t \subseteq \mathcal{U}_t$ , obtain a multicast tree  $\mathcal{T} = \{\mathcal{V}^T, \mathcal{E}^T\}$  such that:

$$\mathbf{P2:} \quad g(\lambda, \mathcal{U}'_t) = \min_{\mathcal{T} \in \Omega(\mathcal{U}'_t)} \lim_{T \rightarrow \infty} \frac{1}{T} \mathbb{E}_{\mathcal{T}} \left[ \sum_{t=0}^T \sum_{u \in \mathcal{U}'_t} \omega_u A_u(t) + \lambda \left( \sum_{t=0}^T C(\mathcal{T}_t) - T\bar{C} \right) \right]. \quad (13)$$

We can observe the equivalence between two subproblems and the problem **DP**. Now we focus on solving these problems.

##### B. Scheduling MDP

The scheduling problem **P1** is a primary problem that aims to select a subset of destinations to update at each time slot. Therefore, we naturally reformulate it as an MDP, denoted as  $\mathcal{M}_1 = \{\mathcal{S}_1, \mathcal{A}_1, \mathbb{P}_1, r_1\}$  and described as follows:

- **States:** Let  $\hat{\mathcal{V}} = \max_{t \in \mathbb{N}_0} |\mathcal{V}_t|$  denote the max number of nodes over  $t$ , the state  $s_t$  is defined as:

$$s_t = \{\mathcal{G}_t, \mathbf{x}_t\}, s_t \in \mathbb{R}^{\hat{\mathcal{V}}^2 + 6\hat{\mathcal{V}}}, \quad (14)$$

where  $\mathbf{x}_t \in \mathbb{R}^{6\hat{\mathcal{V}}}$  denote node features at time  $t$ . The specific information of  $\mathbf{x}_t$  is described in Table I. The topology  $\mathcal{G}_t$  is represented by an adjacency matrix with  $\hat{\mathcal{V}}^2$  elements.

- **Actions:** The action includes all subsets of  $\mathcal{U}_t$ , i.e.:

$$\mathcal{A}_1 = \{\mathcal{U}'_t | \mathcal{U}'_t \subseteq \mathcal{U}_t\}. \quad (15)$$

The action of  $\mathcal{M}_1$  is denoted as  $a_t \in \mathcal{A}_1$ . It is worth noting that the dimension of  $\mathcal{A}_1$  is  $2^{|\mathcal{U}_t|}$ , which is also referred to as the curse of dimensionality [61].

- The transition probability is denoted as  $\mathbb{P}_1$ , which is unknown a priori.
- **Rewards:** The reward function  $r_1$  is defined as:

$$r_1(s_t, a_t) = \sum_{\tau} r_2(s_{\tau}, a_{\tau}), \quad (16)$$

where  $r_2(s_t, a_t)$  is the reward function of  $\mathcal{M}_2(a_t)$ , which will be introduced later.

##### C. Tree-generating MDP

We start with establishing the following equivalent transformation of **P2**:

**Lemma 2.** Given network  $\mathcal{G}_t$  and a set of destinations  $\mathcal{U}'_t \subseteq \mathcal{U}_t$ , the Problem **P2** is equivalent to the following problem:

$$\mathbf{P2-B:} \quad g(\lambda, \mathcal{U}'_t) = \max_{\mathcal{T} \in \Omega(\mathcal{U}'_t)} \sum_{u \in \mathcal{U}'_t} \omega_u \left( 1 - \frac{h_{\mathcal{T}}(u)}{\hat{h}_{\mathcal{G}_t}} \right) A_u(t) - \lambda(C(\mathcal{T}) - \bar{C}), \quad (17)$$

where  $h_{\mathcal{T}}(u)$  is the number of hops between the source and destination  $u$  in  $\mathcal{T}$ , and  $\hat{h}_{\mathcal{G}_t}$  is the length of  $\mathcal{G}_t$ .

The proof of Lemma 2 is given in Appendix B. We note that Lemma 2 is still a combinatorial optimization algorithm and thus NP-hard. Our approach to tackling the tree-generating subproblem **P2-B** is mainly motivated by the greedy meta-algorithm design in [24]. Note that a tree with  $n$  nodes has exactly  $n - 1$  links. Therefore, we can generate a multicast tree by incrementally selecting nodes and links. Specifically, we initiate with an empty subgraph  $\mathcal{P}$ , which is the partial solution of a multicast tree. Then at each step, we greedily select a node  $v$  and an edge to  $\mathcal{P}$ . The node  $v$  is selected from a heuristic quality function, denoted as  $Q(\mathcal{P}, v)$ . It represents the quality of  $\mathcal{P}$  after adding  $v$  to  $\mathcal{P}$ . The above process can be described as follows:

$$\mathcal{P} := (\mathcal{P}, v^*), \text{ where } v^* = \arg \max_{v \in \bar{\mathcal{P}}} Q(\mathcal{P}, v). \quad (18)$$

As described above, we can view the tree-generating process as a sequential decision-making problem that can be formulated as an MDP. Hence, we further reformulate **P2-B** as follows.

To measure the quality of a partial solution  $\mathcal{P}$ , we can transform the objective of **P2-B** into a quality function by substituting  $\mathcal{P}$  for  $\mathcal{T}$ . Next, we formally define the tree-generating MDP. We introduce a virtual timescale  $\tau$  and a partial solution  $\mathcal{P}_\tau = \{\mathcal{V}_\tau^{\mathcal{P}}, \mathcal{E}_\tau^{\mathcal{P}}\}$  with a source node at  $\tau = 0$ . Recall that problem **P2-B** is influenced by the action of  $\mathcal{M}_1$ , i.e., the selected destinations  $a_t \subseteq \mathcal{U}_t$  (see (15)). Given  $a_t$ , an induced MDP  $\mathcal{M}_2(a_t) = \{\mathcal{S}_2, \mathcal{A}_2, \mathbb{P}_2, r_2\}$  is defined as follows:

- **States:** The state  $s_\tau$  is the partial solution  $\mathcal{P}_\tau$ , i.e.:

$$s_\tau = \{\mathcal{P}_\tau\}, s_\tau \in \mathbb{R}^{\hat{\mathcal{V}}^2 + \hat{\mathcal{V}}}. \quad (19)$$

The state  $s_\tau$  includes two indicators for  $\mathcal{V}_\tau^{\mathcal{P}}$  and  $\mathcal{E}_\tau^{\mathcal{P}}$ , respectively. When  $a_t$  is covered by  $\mathcal{P}_\tau$ ,  $s_\tau$  will be a terminal state and  $\mathcal{P}_\tau$  is the generated multicast tree.

- **Actions:** The action space is defined as:

$$\mathcal{A}_2 = \{v | v \in \mathcal{V}_t, v \notin \mathcal{V}_\tau^{\mathcal{P}}, \exists u \in \mathcal{V}_\tau^{\mathcal{P}}, (u, v) \in \mathcal{E}_t\}. \quad (20)$$

This means that the action  $a_\tau \in \mathcal{A}_2$  is to choose a node  $v$  that is not included in  $\mathcal{P}_\tau$  and the node  $v$  should be connected to at least one node  $u$  in  $\mathcal{P}_\tau$ . In other words, each action  $a_\tau \in \mathcal{A}_2$  is a neighbor of the current partial solution  $\mathcal{P}_\tau$ .

- **Transition:** The transition is deterministic here and corresponds to tagging the selected node as the last action.

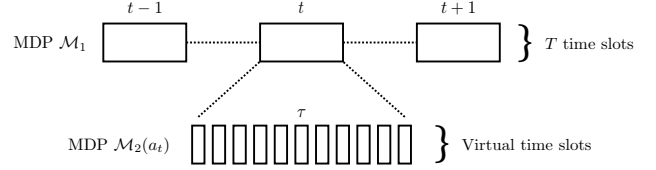


Fig. 3. Temporal relation between two MDPs.  $\mathcal{M}_1$  selects a subset of destinations  $a_t \subseteq \mathcal{U}_t$  at each time slot  $t$ , which is utilized by  $\mathcal{M}_2(a_t)$  to generate multicast trees.  $\tau$  is a virtual timescale that discretizes the generation process of a multicast tree.

- **Rewards:** The quality function  $q_2(s_\tau)$  can be defined as:

$$q_2(s_\tau) = \sum_{u \in \mathcal{U}'_t \cap \mathcal{V}_\tau^{\mathcal{P}}} \omega_u \left( 1 - \frac{h_{\mathcal{P}_\tau}(u)}{\hat{h}_{\mathcal{G}_t}} \right) A_u(t) - \lambda(C(\mathcal{P}_\tau) - W), \quad (21)$$

where  $h_{\mathcal{P}_\tau}(u)$  is the number of hops between the source and destination  $u$  in  $\mathcal{P}_\tau$ , and  $\hat{h}_{\mathcal{G}_t}$  is the length of  $\mathcal{G}_t$ . Subsequently, the reward function  $r_2$  is defined as:

$$r_2(s_\tau, a_\tau) = q_2(s_{\tau+1}) - q_2(s_\tau). \quad (22)$$

When considering a candidate  $a_\tau$  for inclusion in the partial solution, we will choose the link with the lowest cost from the set of candidate links that connect the nodes  $\mathcal{V}_\tau^{\mathcal{P}}$  and node  $a_\tau$ :

$$(v_\tau^*, a_\tau) = \arg \min_{v \in \mathcal{V}_\tau^{\mathcal{P}}, (v, a_\tau) \in \mathcal{E}_\tau^{\mathcal{P}}} C_{v, a_\tau}. \quad (23)$$

This approach effectively reduces the complexity of  $\mathcal{A}_2$  while constraining the cost of  $\mathcal{P}_\tau$ . The following proposition ensures that the generated subgraph is a multicast tree of  $\mathcal{U}'_t$ :

**Proposition 1.** At the terminal state  $s_{\tau'}$  of  $\mathcal{M}_2(a_t)$ ,  $\mathcal{P}_{\tau'}$  is a multicast tree including  $a_t$ .

We present the proof of Proposition 1 in Appendix C.

#### D. Relation between Scheduling and Tree-Generating MDPs

Here, we analyze the relation between  $\mathcal{M}_1$  and  $\mathcal{M}_2(a_t)$ . The temporal relation is illustrated in Fig. 3. This formulation coincides with the MAXQ decomposition [62], where the scheduling subproblem is a primitive subtask and the tree-generating subproblem is an invoked subtask. The hierarchical structure can effectively address the challenges of coupled decision variables. Then we analyze the equivalence between  $\mathcal{M}_1$ ,  $\mathcal{M}_2(a_t)$  and problem **DP**. The equivalence between  $\mathcal{M}_2(a_t)$  and **P2** can be described as follows:

**Lemma 3.** Given a subset of destinations  $\mathcal{U}'_t \subseteq \mathcal{U}_t$ , solving  $\mathcal{M}_2(\mathcal{U}'_t)$  is equivalent to solving problem **P2**.

*Proof.* The cumulative reward of  $\mathcal{M}_2(\mathcal{U}'_t)$  can be denoted as:

$$\begin{aligned} R_2 &= \sum_{\tau} \gamma^\tau r_2(s_\tau, a_\tau) \stackrel{\gamma=1}{=} q_2(s_{\tau'}) - q_2(s_0) \\ &= \sum_{u \in \mathcal{U}'_t} \omega_u \left( 1 - \frac{h_{\mathcal{P}_{\tau'}}(u)}{\hat{h}_{\mathcal{G}_t}} \right) A_u(t) - \lambda(C(\mathcal{P}_{\tau'}) - W), \end{aligned} \quad (24)$$

where  $s_{\tau'}$  is a terminal state. Note that  $\mathcal{P}_{\tau'}$  for  $\mathcal{M}_2(\mathcal{U}_t')$  can be written as  $\mathcal{T}_t$ . Note that the objective of problem **P2-B** is the same as  $R_2$ . In addition, the two problems have the same solution space. Hence, we conclude that solving  $\mathcal{M}_2(\mathcal{U}_t')$  is equivalent to solving **P2-B**. From Lemma 2, the proof is concluded.  $\square$

## V. TREE GENERATOR-BASED MULTICAST SCHEDULING

As mentioned above, the dimensions of  $\mathcal{S}_1$ ,  $\mathcal{A}_1$ , and  $\mathcal{S}_2$  are huge for existing methods to explore. To address this challenge, we propose a Tree Generator-based Multicast Scheduling (TGMS) algorithm. Our proposed approach consists of a tree generator and a scheduler, which utilize graph embedding methods and DRL techniques. The proposed graph embedding method lowers the dimensions from  $\mathcal{O}(\mathcal{V}^2)$  to  $\mathcal{O}(\mathcal{V})$  with key information extracted.

### A. Representation: Graph Embedding Methods

To efficiently solve  $\mathcal{M}_1$  and  $\mathcal{M}_2(a_t)$ , it is crucial to have a deep and comprehensive understanding of the graph's spatial structure, including the relations between nodes and edges. Graph embedding methods (e.g., GNNs) are valuable for extracting graph information and have demonstrated their efficacy in various CO problems [24]. Some studies have focused on the attention mechanism in GNNs, which has the advantage of selectively aggregating information from neighbors (e.g., [63]). Thus, we propose the following GAT:

$$\phi(\mathbf{h}_i, \mathbf{h}_j) = \mathbf{a}^T \text{LeakyReLU}(\mathbf{W}_1(\mathbf{h}_i + \mathbf{h}_j) + \mathbf{W}_2 \mathbf{e}_{i,j}), \quad (25a)$$

$$\alpha_{ij} = \frac{\exp(\phi(\mathbf{h}_i, \mathbf{h}_j))}{\sum_{k \in \mathcal{N}_i \cup \{i\}} \exp(\phi(\mathbf{h}_i, \mathbf{h}_k))}, \quad (25b)$$

$$f_{\text{GAT}}(\mathbf{h}_i, \mathbf{x}) = \frac{1}{\|\mathbf{W}_1\|} (\alpha_{ii}(\mathbf{W}_1 \mathbf{h}_i + \mathbf{W}_3 \mathbf{x}_i) + \sum_{j \in \mathcal{N}_i} \alpha_{ij}(\mathbf{W}_1 \mathbf{h}_j + \mathbf{W}_3 \mathbf{x}_j)), \quad (25c)$$

where  $\mathbf{W}_1$ ,  $\mathbf{W}_2$ , and  $\mathbf{W}_3$  are learnable parameters,  $\mathbf{x} = \{\mathbf{x}_i\}$  denotes the node features,  $\mathbf{e}_{i,j}$  denotes the edge features of edge  $(i, j)$ , and  $\mathbf{h}_i \in \mathbb{R}^d$  denotes the embedding vector of node  $i$ . Note that the new representation of node  $i$  is obtained by a weighted sum of neighbors' embeddings using  $\alpha_{ij}$ , which effectively disseminates information through the graph. An important feature of the above GAT is the contraction mapping property. Let  $d$  be a distance metric for node embeddings, defined as  $d(\mathbf{H}, \mathbf{H}') = \|\sum_{i \in \mathcal{V}} (\mathbf{h}_i - \mathbf{h}'_i)\|$ , where  $\mathbf{H} = \{\mathbf{h}_0, \mathbf{h}_1, \dots\}$  and  $\mathbf{H}' = \{\mathbf{h}'_0, \mathbf{h}'_1, \dots\}$  are the matrices of node embeddings. Then  $f(\cdot, \mathbf{x})$  is a contraction mapping if:

$$d(f(\mathbf{H}, \mathbf{x}), f(\mathbf{H}', \mathbf{x})) \leq d(\mathbf{H}, \mathbf{H}'). \quad (26)$$

Then we have the following theorem:

<sup>1</sup>LeakyReLU( $x$ ) = max( $\alpha x$ ,  $x$ ) where  $\alpha$  is a hyperparameter.

**Theorem 1.** For any undirected graph  $\mathcal{G} = \{\mathcal{V}, \mathcal{E}\}$ , given a mapping  $f_{\text{GAT}}$  defined by (25), if the attention coefficients  $\alpha_{ij}$  are symmetric, i.e.,  $\alpha_{ij} = \alpha_{ji}$ . Then  $f_{\text{GAT}}(\cdot, \mathbf{x})$  is a contraction mapping for any initial node embeddings.

*Proof.* The proof can be found in the appendix of [64].  $\square$

**Remark 3.** (i) According to Banach's fixed-point theorem [65], the mapping  $f_{\text{GAT}}(\mathbf{H}, \mathbf{x})$  has a unique fixed point, meaning that the GAT can map the node features to a stable state; (ii) GAT can be regarded as a dimension-reduction technique with the ability to capture the importance of nodes; (iii) the output of GAT can be perceived as a noisy representation of the network state, which can be effectively leveraged in reinforcement learning (RL) methods.

### B. Learning: Advantage Actor-Critic Algorithm

Our proposed TGMS algorithm consists of two agents: a scheduler and a tree generator. Each agent is learned from the Advantage Actor-Critic (A2C) algorithm [66], including an actor and a critic. Let  $\theta$  denote the parameters of an actor and  $\omega$  denote the parameters of a critic. We consider the following state-value function:

$$v_{\pi_{\theta}}(s) = \mathbb{E}_{\substack{a_t \sim \pi_{\theta}(\cdot | s_t) \\ s_{t+1} \sim \mathbb{P}_{\pi_{\theta}}(\cdot | s_t, a_t)}} \left[ \sum_{t=0}^{\infty} \gamma^t r(s_t, a_t) | s_0 = s \right], \quad (27)$$

where  $\pi_{\theta}$  is the parameterized policy under  $\theta$  and  $\mathbb{P}_{\pi_{\theta}}(\cdot | s_t, a_t)$  is the transition probability under policy  $\pi_{\theta}$ . We aim to maximize the expected state value of the initial state  $s_0$ . The objective function is denoted as  $J(\theta) := v_{\pi_{\theta}}(s_0)$ . To optimize  $\theta$ , we first analyze how action  $a_t$  outperforms other actions under state  $s_t$ . It is measured by the advantage function, denoted as:

$$A_{\pi_{\theta}}(s_t, a_t) = r(s_t, a_t) - v_{\pi_{\theta}}(s_t) \quad (28)$$

According to the policy gradient theorem [67], the gradient of  $J(\theta)$  can be denoted as:

$$\nabla J(\theta) = \mathbb{E}_{s_t \sim \mu_{\theta}, a_t \sim \pi_{\theta}} [A_{\pi_{\theta}}(s_t, a_t) \nabla \log \pi_{\theta}(a_t | s_t)]. \quad (29)$$

However, due to high-dimensional nature of  $\mathcal{M}_1$  and  $\mathcal{M}_2(a_t)$ , it is infeasible to directly access  $v_{\pi_{\theta}}$ . Hence, the critic is used to approximate the value of state  $s_t$ , denoted as  $V_{\omega}(s_t)$ . The pseudo-code of A2C is described in Algorithm 1. The actor is updated by (29) and the critic is updated from the error between  $v_{\pi_{\theta}}$  and  $V_{\omega}(s_t)$ . The following theorem gives the convergence of the above algorithm in our scenario:

**Theorem 2** (Convergence of Algorithm 1). Given the parameter sequence of the critic below:

$$\mathcal{E}(k) = \frac{2}{k} \sum_{i=n}^k \mathbb{E}[\|\omega^* - \omega_i\|^2]. \quad (30)$$

If it is bounded, then we have the following convergence:

$$\min_{n \leq i \leq k} \mathbb{E}[\|\nabla J(\theta_i)\|^2] = \mathcal{O}\left(\frac{\mathcal{E}(k)}{n}\right) + \mathcal{O}\left(\frac{1}{n^{\sigma}}\right) \quad (31)$$



---

**Algorithm 1** Advantage Actor-Critic (A2C)

**Input:** An episode  $\{s_0, a_0, r_0, s_1, a_1, r_1, \dots, s_T, a_T, r_T\}$ 
**Parameter:**  $\theta$  - actor,  $\omega$  - critic

- 1:  $t \leftarrow 0$ .
  - 2: **while**  $t < T$  **do**
  - 3:  $A_t \leftarrow \sum_{k=t}^T \gamma^k r_k - V_\omega(s_t)$ .
  - 4:  $d\theta \leftarrow d\theta + \nabla_{\theta}(\log \pi_{\theta}(a_t|s_t)A_t + H_{\theta})$ .
  - 5:  $d\omega \leftarrow d\omega + \partial(R - V_\omega(s_t))^2 / \partial\omega$ .
  - 6:  $t \leftarrow t + 1$ .
  - 7: **end while**
- 

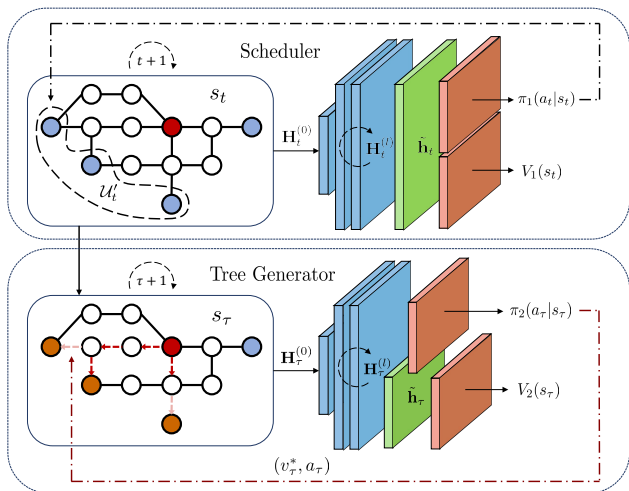


Fig. 4. The system architecture of TGMS. A scheduler is performed to select a set of destinations, which are utilized by the tree generator to generate a multicast tree. The initial graph embedding is fed into GATs (blue blocks) to be iteratively updated. The outputs are passed through a pooling layer (green block) to aggregate global information and then forwarded to two distinct heads (red blocks) for policy and value predictions.

Due to the space limit, the proof can be found in our online technical report [64].

### C. System Architecture

The *system architecture* of TGMS is illustrated in Fig. 4. At each time slot  $t$ , the scheduler selects a subset of destinations  $\mathcal{U}'_t$  from  $\mathcal{U}_t$ . The tree generator is then invoked to generate a multicast tree  $\mathcal{T}_t$  for  $\mathcal{U}'_t$ . The graph is first embedded with GATs (blue blocks) to capture the spatial structure of the network. The outputs are then passed through a pooling layer (green block) to aggregate global information. The resulting graph embeddings are fed into an actor and a critic (red blocks) for policy and value predictions.

Here, we formally describe the *forwarding process* of the scheduler and the tree generator. Recall that the action space of  $\mathcal{M}_1$ , (15), is excessively large, making it impractical for the efficient exploration of classical MDP algorithms. In addition, the size of  $\mathcal{U}_t$  varies across different networks, which further complicates the problem. To address the above challenges, we consider a continuous action output. Specifically, we predict

the mean and standard deviation of the Gaussian distribution for each node. These predictions are then used to sample the destinations. The forwarding process of the scheduler can be summarized as follows:

$$\mathbf{H}_t^{(0)} = s_t, \mathbf{H}_t^{(l+1)} = f_{\text{GAT}}(\{\mathbf{h}_{t,i}^{(l)}\}_{i \in \mathcal{V}_t}, \mathbf{x}_t), \quad (32a)$$

$$\tilde{\mathbf{h}}_t = \frac{1}{|\mathcal{V}|} \sum_{i=1}^{|\mathcal{V}|} \mathbf{h}_t^{(L)}, \quad (32b)$$

$$\mu = \mathbf{W}_1 \text{LeakyReLU}(\mathbf{W}_2 \tilde{\mathbf{h}}_t), \quad (32c)$$

$$\sigma = \mathbf{W}_3 \text{LeakyReLU}(\mathbf{W}_4 \tilde{\mathbf{h}}_t), \quad (32d)$$

$$\pi_1(a_t|s_t) = \mathcal{N}(\mu, \sigma), \quad (32e)$$

$$V_1(s_t) = \mathbf{W}_5 \text{LeakyReLU}(\mathbf{W}_6 \tilde{\mathbf{h}}_t), \quad (32f)$$

where  $\mathcal{N}(\mu, \sigma)$  denotes a Gaussian distribution with mean  $\mu$  and standard deviation  $\sigma$ . The graph embedding is updated by the GAT defined by (25a)-(25c). Following this, the outputs are passed through a pooling layer that aggregates global information (see (32b)). The resulting graph embeddings are fed into two distinct heads: (i) a policy head responsible for predicting  $\mu$  and  $\sigma$  (see (32c)-(32e)); and (ii) a critic head tasked with predicting the value of the state  $s_t$  (see (32f)). For the tree generator, we employ graph embedding methods similar to those used in the scheduler. The difference lies in the heads as follows:

$$\pi_2(a_\tau|s_\tau) = \log \text{softmax}(\mathbf{W}'_1 \sigma(\mathbf{W}'_2 \mathbf{H}_\tau^{(L)})), \quad (33a)$$

$$V_2(s_\tau) = \mathbf{W}'_3 \text{LeakyReLU}(\mathbf{W}'_4 \tilde{\mathbf{h}}_\tau), \quad (33b)$$

where the policy  $\pi_2(a_\tau|s_\tau)$  is masked to ensure valid actions.

The *inference process* of the TGMS is described in Algorithm 2. Given the initial network graph topology and features, the TGMS algorithm iteratively selects a subset of destinations  $\mathcal{U}'_t$  and generates a multicast tree  $\mathcal{T}_t$  for each time slot  $t$ . The scheduling process is performed by the scheduler, which is based on  $\mathcal{M}_1$ . The tree-generating process is invoked to generate a multicast tree for the selected destinations, which is based on  $\mathcal{M}_2(a_t)$ . In the training process, the Lagrangian multiplier  $\lambda$  will be updated.

## VI. EXPERIMENTAL EVALUATION

In this section, we conduct extensive experiments to evaluate the performance of our approach. Due to the lack of existing research on the proposed problem, we consider three different types of graph topologies to validate the robustness of our algorithm. We consider four baseline algorithms and measure their performance using two AoI metrics under different energy constraints.

### A. Environment Settings

The datasets are described below.

- **ER Graphs:** The Erdős-Renyi (ER) random graphs are a type of graph in which each pair of nodes is connected

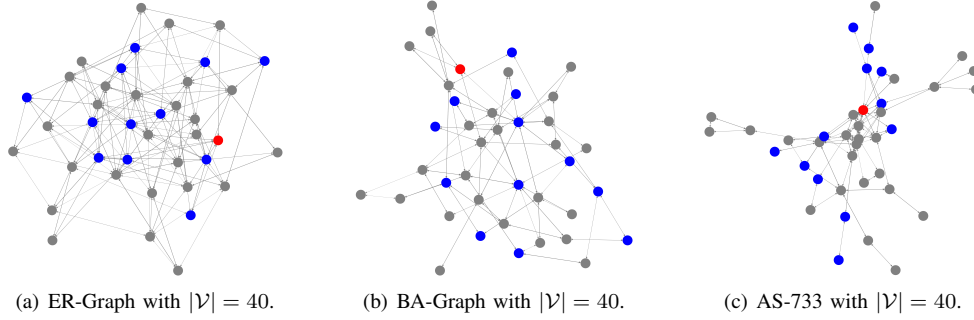


Fig. 5. Graph topology across three datasets. The source node is indicated by the red color, the destination nodes are represented by blue, and the router nodes are depicted in grey.

---

**Algorithm 2** Tree Generator-based Multicast Scheduling (TGMS)

---

**Input:** Network  $\mathcal{G}_0$ , node features  $\mathbf{x}_0$ , and edge features  $\mathbf{e}_0$   
**Output:** Scheduling decisions  $\mathcal{U}' = \{\mathcal{U}'_0, \mathcal{U}'_1, \dots\}$  and multicast trees  $\mathcal{T} = \{\mathcal{T}_0, \mathcal{T}_1, \dots\}$

```

1:  $t \leftarrow 0$ .
2: while  $t < T$  do
3:   Get state  $s_t = \{\mathcal{G}_t, \mathbf{x}_t\}$ .
4:   Compute  $\pi_1(a_t, s_t)$  and  $V_1(s_t)$  from (32).
5:    $\mathcal{U}' \leftarrow$  Sample  $\mathcal{U}'_t \in \mathcal{U}_t$  from  $\pi_1(a_t, s_t)$ .
6:   Initialize  $\tau \leftarrow 0$  and partial solution  $\mathcal{P}_\tau$ .
7:   while  $s_\tau$  is not a terminal state do
8:     Get state  $s_\tau = \{\mathcal{P}_\tau\}$ .
9:     Compute  $\pi_2(a_\tau, s_\tau)$  and  $V_2(s_\tau)$  from (33).
10:    Sample  $a_\tau \in \mathcal{N}(\mathcal{P}_\tau)$  from  $\pi_2(a_\tau, s_\tau)$ .
11:     $\mathcal{P}_\tau \leftarrow$  select a link  $(v_\tau^*, a_\tau)$ .
12:     $\tau \leftarrow \tau + 1$ .
13:   end while
14:    $\mathcal{T} \leftarrow$  Multicast with  $\mathcal{P}_\tau$ .
15:    $\lambda \leftarrow C(\mathcal{T}_t) - W$ .
16:    $t \leftarrow t + 1$ .
17: end while

```

---

with a fixed probability  $p$ . They are widely used in multicast networks (e.g., in [68]).

- **BA Graphs:** In Barabasi-Albert (BA) graphs, each newly introduced node connects to  $m$  pre-existing nodes. The probability is proportional to the number of links existing nodes already possess. These graphs find significant applications within multicast systems (e.g., in [69]).
- **AS-733:** The Autonomous Systems (AS)-733 dataset is a real-world dataset collected from the University of Oregon Route Views Project [70]. It contains 733 abstracted graphs of Autonomous Systems.

Some examples of the above datasets are displayed in Fig. 5. For each dataset, we sample 240 graphs for training and 60 graphs for testing. We set  $|\mathcal{V}_0| = 60$  and randomly select 30% of nodes as destinations. Each graph will be trained or tested for 100 time slots. To simulate a dynamic network, we

resample the graph every 20 time slots when testing.

### B. Baseline Algorithms and Metrics

The following algorithms are considered as baselines:

- **Random:** For the scheduler, we randomly sample a random fraction of destinations. When generating a multicast tree, we first randomly select a valid node from  $\mathcal{A}_2$  and connect it to  $\mathcal{P}_\tau$  with its minimum-cost link.
- **Greedy:** For the scheduler, we greedily select a fraction of destinations that are sorted by their weighted AoI. When generating a multicast tree, we greedily select a valid link with minimum cost from all valid links.
- **TGMS-MLP:** In this method, only the Multilayer Perceptron (MLP) is included in the net. That means we do not use graph embedding methods for the TGMS algorithm.
- **Minimum Spanning Tree (MST):** We adopt Kruskal's algorithm [71] to generate an MST to minimize the sum of edge costs. Note that the energy constraint  $\bar{C}$  is not satisfied by this algorithm.

We consider the following AoI metrics:

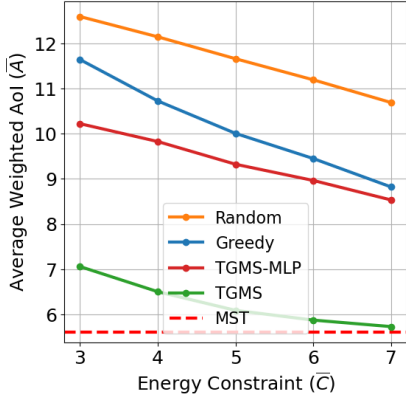
- **Average Weighted AoI:** The main metric of our considered problem is the weighted average-age in (6).
- **Weighted Peak Age:** The weighted peak age is:

$$\bar{A}_{peak} = \limsup_{N \rightarrow \infty} \frac{1}{N} \sum_{p=1}^N \sum_{u \in \mathcal{U}_t} \omega_u A_u(T_u(p)), \quad (34)$$

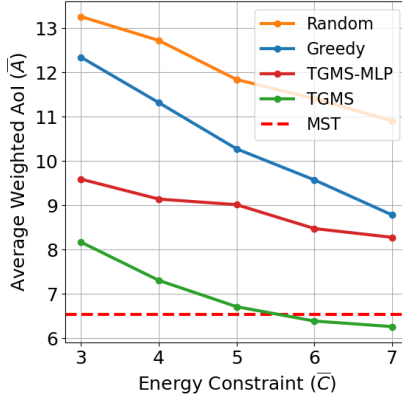
where  $T_u(p)$  denotes the time at which  $u$  receives the  $p$ th update. The peak age is the average of age peaks, which happen just before a packet arrives.

### C. Experiment Results

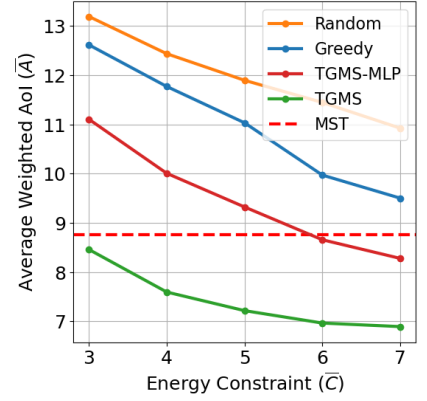
For each dataset, we consider a set of different energy constraints  $\bar{C} \in \{3, 4, 5, 6, 7\}$  and compare the AoI metrics. The results are shown in Figs. 6 and 7. From Fig. 6, we observe that TGMS performs superiorly to the baselines for all datasets. While TGMS-MLP performs better than the Random and the Greedy, it can not efficiently extract the graph information. Although MST also yields a low average weighted



(a) Average Weighted AoI of AS-733.

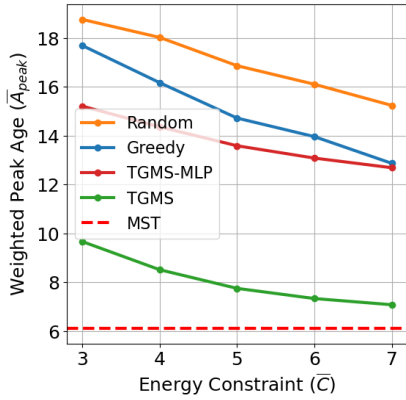


(b) Average Weighted AoI of BA Graphs.

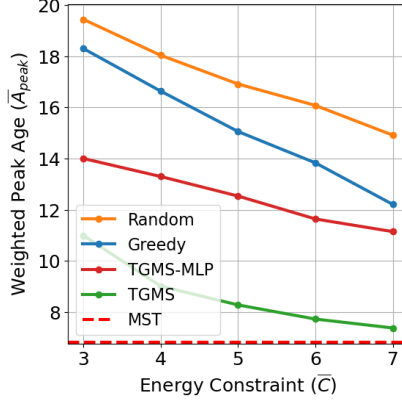


(c) Average Weighted AoI of ER Graphs.

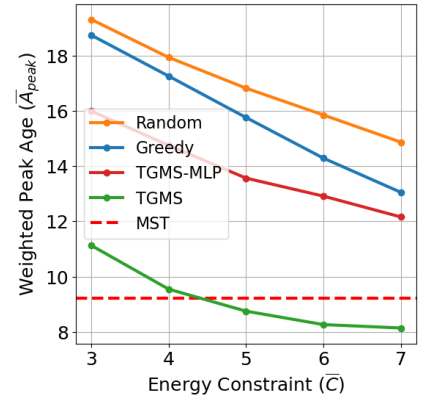
Fig. 6. Average weighted AoI over three datasets with  $|\mathcal{V}| = 60$ . While MST yields a low average weighted AoI, the average energy consumption for three datasets is 27.18, 20.70, and 18.63, respectively.



(a) Peak Weighted Age of AS-733.



(b) Peak Weighted Age of BA Graphs.



(c) Peak Weighted Age of ER Graphs.

Fig. 7. Peak weighted age over three datasets with  $|\mathcal{V}| = 60$ .

AoI compared with TGMS, the average energy consumption for three datasets is 27.18, 20.70, and 18.63, respectively, which do not satisfy the given energy constraints. Compared with other baselines, TGMS reduces the average weighted AoI by 39.8%, 33.4%, and 31.3% over three datasets. From Fig. 7, TGMS reduces the peak weighted age by 47.2%, 41.9%, and 41.1%, respectively. It means that TGMS is a fair and robust multicast algorithm over various graph topologies. The additional experiments (e.g., performance on larger graphs) can be found in [64].

## VII. CONCLUSIONS

In this paper, we have formulated the first AoI-optimal multicast problem via joint scheduling and routing. We have applied an RL framework to learn the heuristics of multicast routing, based on which we have performed problem decomposition amenable to hierarchical RL methods. We have further proposed a novel GAT with the contraction property to extract the graph information. Experimental results have demonstrated

that TGMS offers advantages over other benchmarks, including non-cross-layer design, existing multicast algorithms, and methods without graph embedding.

Interesting future directions for research include exploring the consideration of multi-source multicast and the decentralized implementation of the proposed algorithm via multi-agent RL.

## APPENDIX

### A. Model Setting

The parameters for the scheduler, tree generator, and Lagrangian multiplier are shown in Table II, III and IV, respectively. The unit of training interval is the time slot. We use PyGraph 2.4.0 to implement TGMS, which is trained on NVIDIA GeForce RTX 3090 and tested on AMD EPYC 7763 CPU @1.50GHz with 64 cores under Ubuntu 20.04.6 LTS.

TABLE II  
SCHEDULER SETTING

Module	Parameter	Value
A2C	Training Interval	20
	Discount factor ( $\gamma$ )	0.99
	Hidden dimensions	64
Network	Attention heads	5
	Dropout rate	0.3
Optimizer	Type	AdamW
	Actor Learning Rate	$2 \times 10^{-6}$
	Critic Learning Rate	$8 \times 10^{-7}$
	Momentum	0.9
	Centered gradient	True
	Gradient norm	0.5
LR Scheduler	Type	CosineAnnealing
	Warm restarts	True
	$T_0$	2
	$T_{mult}$	10
	$\eta_{min}$	$10^{-8}$

TABLE III  
TREE GENERATOR SETTING

Module	Parameter	Value
A2C	Training Interval	1
	Discount factor ( $\gamma$ )	0.99
	Hidden dimensions	64
Network	Attention heads	5
	Dropout rate	0.3
Optimizer	Type	AdamW
	Actor Learning Rate	$10^{-6}$
	Critic Learning Rate	$4 \times 10^{-7}$
	Momentum	0.9
	Centered gradient	True
	Gradient norm	0.5
LR Scheduler	Type	CosineAnnealing
	Warm restarts	True
	$T_0$	2
	$T_{mult}$	10
	$\eta_{min}$	$10^{-8}$

TABLE IV  
LAGRANGIAN MULTIPLIER SETTING

Parameter	Value
Init Value	0.05
Training Interval	100
Learning Rate	$10^{-5}$

### B. Proof of Lemma 2

We first analyze the relation between multicast tree  $\mathcal{T}_t$  and AoI reduction:

**Lemma 4.** Given a multicast tree  $\mathcal{T}_t$ , if there are no other transmitting packets, the average AoI reduction of destination  $u$  caused by  $\mathcal{T}_t$  is  $\frac{A_u(t)}{h_{\mathcal{T}_t}(u)}$  during time  $[t, t + h_{\mathcal{T}_t}(u)]$ .

*Proof.* Denote  $\Delta A_u(t, t + h_{\mathcal{T}_t}(u))$  as the AoI reduction of

destination  $u$  during time  $[t, t + h_{\mathcal{T}_t}(u)]$ , we have:

$$\begin{aligned}
& \Delta A_u(t, t + h_{\mathcal{T}_t}(u)) \\
&= A_u^+(t, t + h_{\mathcal{T}_t}(u)) - A_u^-(t, t + h_{\mathcal{T}_t}(u)) \\
&= \sum_{k=0}^{h_{\mathcal{T}_t}(u)} (A_u(t) + k) - \left( \sum_{k=0}^{h_{\mathcal{T}_t}(u)-1} (A_u(t) + k) + h_{\mathcal{T}_t}(u) \right) \\
&= A_u(t),
\end{aligned} \tag{35}$$

where  $A_u^+(t, t + h_{\mathcal{T}_t}(u))$  and  $A_u^-(t, t + h_{\mathcal{T}_t}(u))$  denote the AoI of destination  $u$  during time  $[t, t + h_{\mathcal{T}_t}(u)]$  before and after the multicast tree  $\mathcal{T}_t$  is generated, respectively.  $\square$

From the multicast process, we know that the influence of any multicast tree lasts until the packet with maximum hops is received or dropped. Denote  $\hat{h}_{\mathcal{G}_t}$  as the length of  $\mathcal{G}_t$ , we can rewrite the objective of problem **P2** as:

$$g(\lambda, \mathcal{U}'_t) = \max_{\mathcal{T}} \frac{1}{\hat{h}_{\mathcal{G}_t}} \sum_{u \in \mathcal{U}'_t} \sum_{k=0}^{h_{\mathcal{T}}(u)} -\omega_u A_u(t + k) - \lambda(C(\mathcal{T}) - \bar{C}). \tag{36}$$

From the first term of RHS of (36) in Lemma 4, we have:

$$\begin{aligned}
& \max_{\mathcal{T}} \frac{1}{\hat{h}_{\mathcal{G}_t}} \sum_{u \in \mathcal{U}'_t} \sum_{k=0}^{\hat{h}_{\mathcal{G}_t}} -\omega_u A_u(t + k) \\
&= \max_{\mathcal{T}} \frac{1}{\hat{h}_{\mathcal{G}_t}} \sum_{u \in \mathcal{U}'_t} \omega_u \sum_{k=0}^{\hat{h}_{\mathcal{G}_t}} (A_u(t) + k - A_u(t + k)) \\
&= \max_{\mathcal{T}} \frac{1}{\hat{h}_{\mathcal{G}_t}} \sum_{u \in \mathcal{U}'_t} \omega_u \sum_{k=h_{\mathcal{T}}(u)}^{\hat{h}_{\mathcal{G}_t}} (A_u(t) + k - A_u(t + k)) \tag{37} \\
&= \max_{\mathcal{T}} \frac{1}{\hat{h}_{\mathcal{G}_t}} \sum_{u \in \mathcal{U}'_t} \omega_u (\hat{h}_{\mathcal{G}_t} - h_{\mathcal{T}}(u)) A_u(t) \\
&= \max_{\mathcal{T}} \sum_{u \in \mathcal{U}'_t} \left( 1 - \frac{h_{\mathcal{T}}(u)}{\hat{h}_{\mathcal{G}_t}} \right) \omega_u A_u(t).
\end{aligned}$$

Substitute (37) into (36) concludes the proof.

### C. Proof of Proposition 1

From the definition of the action space  $\mathcal{A}_2$ , the chosen node  $a_{\tau'} \in \mathcal{A}_2$  is connected to  $\mathcal{P}_{\tau'}$  and is not chosen before, which means  $\mathcal{P}_{\tau'}$  is connected and acyclic. Therefore,  $\mathcal{P}_{\tau'}$  is a tree. In addition,  $\mathcal{P}_{\tau'}$  is initialized with a source node. From the definition of a terminal state  $s_{\tau'}$ ,  $a_t$  is included in  $\mathcal{P}_{\tau'}$ . Therefore,  $\mathcal{P}_{\tau'}$  is a multicast tree.

#### D. Proof of Theorem 1

Given any two node embeddings  $\mathbf{H}$  and  $\mathbf{H}'$ . From (25c), we have:

$$\begin{aligned}
& d(f_{\text{GAT}}(\mathbf{H}, \mathbf{x}), f_{\text{GAT}}(\mathbf{H}', \mathbf{x})) \\
&= \left\| \sum_{i \in \mathcal{V}} (f_{\text{GAT}}(\mathbf{h}_i, \mathbf{x}) - f_{\text{GAT}}(\mathbf{h}'_i, \mathbf{x})) \right\| \\
&= \left\| \sum_{i \in \mathcal{V}} \frac{1}{\|\mathbf{W}_1\|} (\alpha_{ii}(\mathbf{W}_1 \mathbf{h}_i + \mathbf{W}_3 \mathbf{x}_i) \right. \\
&\quad \left. + \sum_{j \in \mathcal{N}_i} \alpha_{ij}(\mathbf{W}_1 \mathbf{h}_j + \mathbf{W}_3 \mathbf{x}_j) - \alpha_{ii}(\mathbf{W}_1 \mathbf{h}'_i + \mathbf{W}_3 \mathbf{x}_i) \right. \\
&\quad \left. - \sum_{k \in \mathcal{N}_i} \alpha_{ik}(\mathbf{W}_1 \mathbf{h}'_k + \mathbf{W}_3 \mathbf{x}_k) \right\| \\
&= \frac{1}{\|\mathbf{W}_1\|} \left\| \sum_{i \in \mathcal{V}} (\alpha_{ii} \mathbf{W}_1 (\mathbf{h}_i - \mathbf{h}'_i) + \sum_{j \in \mathcal{N}_i} \alpha_{ij} \mathbf{W}_1 \mathbf{h}_j \right. \\
&\quad \left. - \sum_{k \in \mathcal{N}_i} \alpha_{ik} \mathbf{W}_1 \mathbf{h}'_k \right\| \\
&= \frac{1}{\|\mathbf{W}_1\|} \left\| \mathbf{W}_1 \sum_{i \in \mathcal{V}} (\alpha_{ii} (\mathbf{h}_i - \mathbf{h}'_i) + \sum_{k \in \mathcal{D}_i} \alpha_{ki} (\mathbf{h}_i - \mathbf{h}'_i)) \right\| \\
&\stackrel{\alpha_{ij}=\alpha_{ji}}{=} \frac{1}{\|\mathbf{W}_1\|} \left\| \mathbf{W}_1 \sum_{i \in \mathcal{V}} (\alpha_{ii} + \sum_{k \in \mathcal{D}_i} \alpha_{ik}) (\mathbf{h}_i - \mathbf{h}'_i) \right\| \\
&= \frac{1}{\|\mathbf{W}_1\|} \left\| \mathbf{W}_1 \sum_{i \in \mathcal{V}} (\alpha_{ii} + \sum_{j \in \mathcal{N}_i} \alpha_{ij}) (\mathbf{h}_i - \mathbf{h}'_i) \right\| \\
&\leq \left\| \sum_{i \in \mathcal{V}} (\mathbf{h}_i - \mathbf{h}'_i) \right\| = d(\mathbf{H}, \mathbf{H}').
\end{aligned} \tag{38}$$

#### E. Proof of Theorem 2

We consider a model consisting of GAT layers and linear layers. Denote  $\mathbf{H}^*$  as the fixed point of GAT, we can view the output of GAT as a new representation of the network state. For simplicity, let  $s = \mathbf{H}^*$  denote the new state. We can then analyze the linear part of the heads. Let  $\theta$  and  $\omega$  be the parameters of the actor and the critic, respectively. We first introduce some assumptions as follows.

**Assumption 2.** Suppose all reward functions  $r$  and the parameterized policy  $\pi_\theta$  satisfy the following conditions:

(a)  $r$  is bounded, i.e.:

$$-R \leq r(s, a) \leq R, \forall (s, a) \in \mathcal{S} \times \mathcal{A}. \tag{39}$$

(b)  $\nabla \log \pi_\theta(a|s)$  is  $L_\theta$ -Lipschitz and bounded<sup>2</sup>, i.e.:

$$\|\nabla \log \pi_{\theta_1}(a|s) - \nabla \log \pi_{\theta_2}(a|s)\| \leq L_\theta \|\theta_1 - \theta_2\|, \tag{40}$$

$$\|\nabla \log \pi_\theta(a|s)\| \leq B_\theta, \forall \theta_1, \theta_2 \in \mathbb{R}^d, \tag{41}$$

where  $L_\theta, B_\theta$  are constants.

**Assumption 3.** Suppose the critic satisfies the following condition:

<sup>2</sup>The gradient of the policy is bounded by the gradient clipping technique.

(a) The critic can be represented by a linear function  $V_\omega(s) = \phi(s)^\top \omega$ , where  $\phi(s)$  is the feature vector of state  $s$  and  $\omega$  is the parameter of the critic.

(b) The feature mapping  $\phi(s)$  has a bounded norm  $|\phi(s)| \leq 1$ .

(c)  $V_\omega(s)$  is bounded, i.e.:  $|V_\omega(s)| \leq B_\omega$ , where  $B_\omega$  is a constant.

The assumption 3 holds due to the contraction mapping of the GAT. For the objective function  $J(\theta)$ , we have  $|J(\theta)| < \frac{R}{1-\gamma}$ . As Assumption 3 states, we can obtain an approximated advantage value function  $\hat{A}_t(s_t, a_t) = r(s_t, a_t) - V_\omega(s_t)$ , where  $\omega$  is the parameter of the critic. Then the gradient of  $J(\theta)$  can be approximated by:

$$\nabla \hat{J}(\theta) = \mathbb{E}_{s \sim \mu_\theta, a \sim \pi_\theta} [\hat{A}_{\pi_\theta}(s, a) \nabla \log \pi_\theta(a|s)], \tag{42}$$

and  $\nabla \hat{J}(\theta)$  is bounded as follows:

**Lemma 5** (Bound of Approximated Policy Gradient). Under Assumption 2 and 3, the policy gradient  $\nabla \hat{J}(\theta)$  is bounded, i.e.:

$$\|\nabla \hat{J}(\theta)\| \leq (R + B_\omega) B_\theta. \tag{43}$$

*Proof.* The approximated advantage value function  $\hat{A}_t(s_t, a_t)$  can be written as:

$$\begin{aligned}
\hat{A}_t(s_t, a_t) &= r(s_t, a_t) - \phi(s_t)^\top \omega \\
&\leq |r(s_t, a_t)| + |\phi(s_t)^\top \omega| \leq R + B_\omega,
\end{aligned} \tag{44}$$

which implies:

$$\|\hat{A}_t(s_t, a_t) \nabla \log \pi_\theta(a_t|s_t)\| \leq (R + B_\omega) B_\theta. \tag{45}$$

The proof is concluded.  $\square$

Now we analyze the approximation error of  $\nabla \hat{J}(\theta)$ . First, introduce the following lemma:

**Lemma 6** (Lipschitz-Continuity of Policy Gradient [72]). Under Assumption 2, the policy gradient  $\nabla J(\theta)$  is Lipschitz continuous with some constant  $L > 0$ , i.e.:

$$\|\nabla J(\theta_1) - \nabla J(\theta_2)\| \leq L \|\theta_1 - \theta_2\|. \tag{46}$$

According to Lemma 6 and (1.2.19) from [73], we have:

$$J(\theta_2) \geq J(\theta_1) + \langle \nabla J(\theta_1), \theta_2 - \theta_1 \rangle - \frac{L}{2} \|\theta_1 - \theta_2\|^2, \tag{47}$$

where  $\langle \cdot, \cdot \rangle$  denotes the dot product of two vectors. The actor of Algorithm 1 is updated by:

$$\theta_{t+1}^a = \theta_t^a + \alpha_t \hat{A}_t(s_t, a_t) \nabla \log \pi_{\theta_t}(a_t|s_t), \tag{48}$$

Substitute (48) into (47) yields:

$$J(\theta_{t+1}) \geq J(\theta_t) + \alpha_t \langle \nabla J(\theta_t), \nabla \hat{J}(\theta_t) \rangle - \frac{L \alpha_t^2}{2} \|\nabla \hat{J}(\theta_t)\|^2. \tag{49}$$

Here, we focus on the second term on the right-hand side of the equation above, which can be decomposed as:

$$\begin{aligned}
& \langle \nabla J(\boldsymbol{\theta}_t), \nabla \hat{J}(\boldsymbol{\theta}_t) \rangle \\
&= \langle \nabla J(\boldsymbol{\theta}_t), \phi(s_t)^\top (\boldsymbol{\omega}^* - \boldsymbol{\omega}_t) \nabla \log \pi_{\boldsymbol{\theta}_t}(a_t | s_t) \rangle \\
&+ \langle \nabla J(\boldsymbol{\theta}_t), (v(s_t) - \phi(s_t)^\top \boldsymbol{\omega}^*) \nabla \log \pi_{\boldsymbol{\theta}_t}(a_t | s_t) \rangle \\
&+ \langle \nabla J(\boldsymbol{\theta}_t), \nabla \hat{J}(\boldsymbol{\theta}_t) - \nabla J(\boldsymbol{\theta}_t) \rangle + \langle \nabla J(\boldsymbol{\theta}_t), \nabla J(\boldsymbol{\theta}_t) \rangle
\end{aligned} \tag{50}$$

We can view the first term on the RHS of (50) as the error of the critic, the second term as the error from linear function approximation of the critic, and the third term as the Markovian noise. Therefore, the above equation can be rewritten as:

$$\begin{aligned}
& \langle \nabla J(\boldsymbol{\theta}_t), \nabla \hat{J}(\boldsymbol{\theta}_t) \rangle \\
&= \Phi_{EC}(\boldsymbol{\theta}_t) + \Phi_{LFA}(\boldsymbol{\theta}_t) + \Phi_M(\boldsymbol{\theta}_t) + \|\nabla J(\boldsymbol{\theta}_t)\|^2,
\end{aligned} \tag{51}$$

We will analyze the bounds of these terms in the following. First,  $\Phi_{EC}(\boldsymbol{\theta}_t)$  measures the distance between the optimal parameter  $\boldsymbol{\omega}^*$  and the current parameter  $\boldsymbol{\omega}_t$ , which is bounded as follows:

**Lemma 7** (Error of Critic). Given Assumption 3, we have:

$$\mathbb{E}[\Phi_{EC}(\boldsymbol{\theta}_t)] \geq -B_\theta \sqrt{\mathbb{E}[\|\nabla J(\boldsymbol{\theta}_t)\|^2]} \sqrt{\mathbb{E}[\|\boldsymbol{\omega}^* - \boldsymbol{\omega}_t\|^2]} \tag{52}$$

*proof:* From Cauchy inequality and (41), we have:

$$\begin{aligned}
& \langle \nabla J(\boldsymbol{\theta}_t), \phi(s_t)^\top (\boldsymbol{\omega}^* - \boldsymbol{\omega}_t) \nabla \log \pi_{\boldsymbol{\theta}_t}(a_t | s_t) \rangle \\
&\geq -\|\nabla J(\boldsymbol{\theta}_t)\| \|\phi(s_t)^\top (\boldsymbol{\omega}^* - \boldsymbol{\omega}_t)\| \|\nabla \log \pi_{\boldsymbol{\theta}_t}(a_t | s_t)\| \\
&\geq -\|\nabla J(\boldsymbol{\theta}_t)\| \|\boldsymbol{\omega}^* - \boldsymbol{\omega}_t\| \|\nabla \log \pi_{\boldsymbol{\theta}_t}(a_t | s_t)\| \\
&\geq -B_\theta \|\nabla J(\boldsymbol{\theta}_t)\| \|\boldsymbol{\omega}^* - \boldsymbol{\omega}_t\|.
\end{aligned} \tag{53}$$

Taking the expectations of both sides yields the result.  $\square$

Then we analyze the approximation error between the optimal parameter  $\boldsymbol{\omega}^*$  and the parameter  $\boldsymbol{\omega}_t$ . Suppose there is an approximation error bound  $\epsilon_v > 0$  that  $\|\mathbb{E}[\phi(s)^\top \boldsymbol{\omega}^* - v(s)]\| \leq \epsilon_v$ , we have:

**Lemma 8** (Error of Linear Function Approximation).

$$\mathbb{E}[\Phi_{LFA}(\boldsymbol{\theta}_t)] \geq -\epsilon_v B_\theta \mathbb{E}[\|\nabla J(\boldsymbol{\theta}_t)\|]. \tag{54}$$

*proof:* From Cauchy inequality, we have:

$$\begin{aligned}
& \langle \nabla J(\boldsymbol{\theta}_t), (v(s_t) - \phi(s_t)^\top \boldsymbol{\omega}^*) \nabla \log \pi_{\boldsymbol{\theta}_t}(a_t | s_t) \rangle \\
&\geq -\|\nabla J(\boldsymbol{\theta}_t)\| \|v(s_t) - \phi(s_t)^\top \boldsymbol{\omega}^*\| \|\nabla \log \pi_{\boldsymbol{\theta}_t}(a_t | s_t)\| \\
&\geq -\epsilon_v B_\theta \|\nabla J(\boldsymbol{\theta}_t)\|.
\end{aligned} \tag{55}$$

Taking the expectations of both sides yields the result.  $\square$

Suppose the Markovian noise is bounded, i.e., there exists  $\epsilon_m > 0$  that  $-\epsilon_m \leq \Phi_M(\boldsymbol{\theta}_t) \leq \epsilon_m$ . Substitute the inequalities above into (51) yields:

$$\begin{aligned}
& \mathbb{E}[\langle \nabla J(\boldsymbol{\theta}_t), \nabla \hat{J}(\boldsymbol{\theta}_t) \rangle] \\
&\geq -B_\theta \sqrt{\mathbb{E}[\|\nabla J(\boldsymbol{\theta}_t)\|^2]} \sqrt{\mathbb{E}[\|\boldsymbol{\omega}^* - \boldsymbol{\omega}_t\|^2]} \\
&- \epsilon_v B_\theta \mathbb{E}[\|\nabla J(\boldsymbol{\theta}_t)\|] - \epsilon_m + \mathbb{E}[\|\nabla J(\boldsymbol{\theta}_t)\|^2].
\end{aligned} \tag{56}$$

Substitute (56) into (49) and take the expectation of both sides yields:

$$\begin{aligned}
& \mathbb{E}[J(\boldsymbol{\theta}_{t+1}) - J(\boldsymbol{\theta}_t)] \\
&\geq -\alpha_t B_\theta \sqrt{\mathbb{E}[\|\nabla J(\boldsymbol{\theta}_t)\|^2]} \sqrt{\mathbb{E}[\|\boldsymbol{\omega}^* - \boldsymbol{\omega}_t\|^2]} \\
&- \alpha_t \epsilon_v \mathbb{E}[\|\nabla J(\boldsymbol{\theta}_t)\|] - \alpha_t \epsilon_m + \alpha_t \mathbb{E}[\|\nabla J(\boldsymbol{\theta}_t)\|^2] - \frac{L\alpha_t^2 B_j^2}{2},
\end{aligned} \tag{57}$$

where  $B_j = (R + B_\omega)B_\theta$ . Rearrange the terms and divide both sides by  $\alpha_t$  yields:

$$\begin{aligned}
& (\mathbb{E}[\|\nabla J(\boldsymbol{\theta}_t)\|] - \frac{\epsilon_v}{2})^2 \leq \frac{1}{\alpha_t} \mathbb{E}[J(\boldsymbol{\theta}_{t+1}) - J(\boldsymbol{\theta}_t)] \\
&+ B_\theta \sqrt{\mathbb{E}[\|\nabla J(\boldsymbol{\theta}_t)\|^2]} \sqrt{\mathbb{E}[\|\boldsymbol{\omega}^* - \boldsymbol{\omega}_t\|^2]} + \frac{L\alpha_t B_j^2}{2} \\
&+ \epsilon_m + \frac{\epsilon_v^2}{4}.
\end{aligned} \tag{58}$$

Summing both sides over  $k$  from  $\tau$  to  $t$ , we have:

$$\begin{aligned}
& \sum_{k=\tau}^t (\mathbb{E}[\|\nabla J(\boldsymbol{\theta}_k)\|] - \frac{\epsilon_v}{2})^2 \leq \sum_{k=\tau}^t \frac{1}{\alpha_k} \mathbb{E}[J(\boldsymbol{\theta}_{k+1}) - J(\boldsymbol{\theta}_k)] \\
&+ B_\theta \sum_{k=\tau}^t \sqrt{\mathbb{E}[\|\nabla J(\boldsymbol{\theta}_k)\|^2]} \sqrt{\mathbb{E}[\|\boldsymbol{\omega}^* - \boldsymbol{\omega}_k\|^2]} \\
&+ \frac{LB_j^2}{2} \sum_{k=\tau}^t \alpha_k + (t - \tau + 1) \left( \epsilon_m + \frac{\epsilon_v^2}{4} \right).
\end{aligned} \tag{59}$$

For the first term of RHS of (59), we have:

$$\begin{aligned}
& \sum_{k=\tau}^t \frac{1}{\alpha_k} \mathbb{E}[J(\boldsymbol{\theta}_{k+1}) - J(\boldsymbol{\theta}_k)] \\
&= \sum_{k=\tau}^{t-1} \left( \frac{1}{\alpha_k} - \frac{1}{\alpha_{k+1}} \right) \mathbb{E}[J(\boldsymbol{\theta}_{k+1})] - \frac{1}{\alpha_\tau} \mathbb{E}[J(\boldsymbol{\theta}_\tau)] \\
&+ \frac{1}{\alpha_t} \mathbb{E}[J(\boldsymbol{\theta}_{t+1})] \\
&\leq \sum_{k=\tau}^{t-1} \left( \frac{1}{\alpha_k} - \frac{1}{\alpha_{k+1}} \right) \frac{R}{1-\gamma} + \frac{1}{\alpha_\tau} \frac{R}{1-\gamma} + \frac{1}{\alpha_t} \frac{R}{1-\gamma} \\
&= \frac{2R}{\alpha_\tau(1-\gamma)}
\end{aligned} \tag{60}$$

Choose  $\alpha_t = c_\alpha / (1+t)^\sigma$  and substitute it into the above equation yields:

$$\begin{aligned}
& \frac{LB_j^2}{2} \sum_{k=\tau}^t \alpha_k \leq \frac{LB_j^2}{2} \sum_{k=0}^{t-\tau} \alpha_k = \frac{LB_j^2 c_\alpha}{2} \sum_{k=0}^{t-\tau} \frac{1}{(1+k)^\sigma} \\
&\leq \frac{LB_j^2 c_\alpha}{2} \int_0^{t-\tau+1} x^{-\sigma} dx \leq \frac{LB_j^2 c_\alpha}{2(1-\sigma)} (t-\tau+1)^{1-\sigma}
\end{aligned} \tag{61}$$

Substitute the above two inequalities into (59) and divide both sides by  $t - \tau + 1$ , we have:

$$\begin{aligned} & \frac{1}{t - \tau + 1} \sum_{k=\tau}^t (\mathbb{E} \|\nabla J(\boldsymbol{\theta}_k)\| - \frac{\epsilon_v}{2})^2 \\ & \leq \frac{B_\theta}{t - \tau + 1} \sum_{k=\tau}^t \sqrt{\mathbb{E}[\|\nabla J(\boldsymbol{\theta}_k)\|^2]} \sqrt{\mathbb{E}[\|\boldsymbol{\omega}^* - \boldsymbol{\omega}_k\|^2]} \\ & + \frac{2R}{\alpha_\tau(1-\gamma)(t-\tau+1)} + \frac{LB_j^2 c_\alpha}{2(1-\sigma)} \frac{1}{(t-\tau+1)^\sigma} \\ & + \epsilon_m + \frac{\epsilon_v^2}{4}. \end{aligned} \quad (62)$$

Assume  $t > 2\tau - 1$ , two terms on the RHS of (62) can be bounded as follows:

$$\begin{aligned} \frac{2R}{\alpha_\tau(1-\gamma)(t-\tau+1)} &= \frac{2c_\alpha R}{(1+\tau)^\sigma(t-\tau+1)} \leq \frac{2c_\alpha R}{(1+\tau)^\sigma \tau} \\ \frac{LB_j^2 c_\alpha}{2(1-\sigma)} \frac{1}{(t-\tau+1)^\sigma} &\leq \frac{LB_j^2 c_\alpha}{2(1-\sigma)} \frac{1}{\tau^\sigma} \end{aligned} \quad (63)$$

$$\frac{LB_j^2 c_\alpha}{2(1-\sigma)} \frac{1}{(t-\tau+1)^\sigma} \leq \frac{LB_j^2 c_\alpha}{2(1-\sigma)} \frac{1}{\tau^\sigma} \quad (64)$$

Here, we analyze the first term on the RHS of (62). By Cauchy-Schwarz inequality, we have:

$$\begin{aligned} & \frac{B_\theta}{t - \tau + 1} \sum_{k=\tau}^t \sqrt{\mathbb{E}[\|\nabla J(\boldsymbol{\theta}_k)\|^2]} \sqrt{\mathbb{E}[\|\boldsymbol{\omega}^* - \boldsymbol{\omega}_k\|^2]} \\ & \leq \frac{B_\theta}{t - \tau + 1} \sqrt{\sum_{k=\tau}^t \mathbb{E}[\|\nabla J(\boldsymbol{\theta}_k)\|^2]} \sqrt{\sum_{k=\tau}^t \mathbb{E}[\|\boldsymbol{\omega}^* - \boldsymbol{\omega}_k\|^2]} \end{aligned} \quad (65)$$

Assume the bound of approximation error of the critic  $\epsilon_v$  satisfies  $\epsilon_v < 2\mathbb{E}[\|\nabla J(\boldsymbol{\theta}_k)\|]$ , substitute it into LHS of (62) yields:

$$\begin{aligned} & \frac{1}{t - \tau + 1} \sum_{k=\tau}^t (\mathbb{E} \|\nabla J(\boldsymbol{\theta}_k)\| - \frac{\epsilon_v}{2})^2 \\ & \leq \frac{1}{t - \tau + 1} \sum_{k=\tau}^t \mathbb{E} \|\nabla J(\boldsymbol{\theta}_k)\|^2 \end{aligned} \quad (66)$$

Denote  $X(t) := 1/(t - \tau + 1) \sum_{k=\tau}^t \mathbb{E}[\|\nabla J(\boldsymbol{\theta}_k)\|^2]$  and  $Y(t) := 1/(t - \tau + 1) \sum_{k=\tau}^t \mathbb{E}[\|\boldsymbol{\omega}^* - \boldsymbol{\omega}_k\|^2]$ , put the above inequalities into (62) yields:

$$X(t) \leq 2B_\theta \sqrt{X(t)} \sqrt{Y(t)} + \mathcal{O}\left(\frac{1}{\tau^\sigma}\right), \quad (67)$$

which is equivalent to:

$$(\sqrt{X(t)} - B_\theta \sqrt{Y(t)})^2 \leq \mathcal{O}\left(\frac{1}{\tau^\sigma}\right) + B_\theta^2 Y(t). \quad (68)$$

According to the monotonicity of the square root function, we have:

$$\sqrt{X(t)} \leq \sqrt{\mathcal{O}\left(\frac{1}{\tau^\sigma}\right) + 2B_\theta \sqrt{Y(t)}}. \quad (69)$$

Note that if  $A < B + C$  and A, B, C are non-negative, then  $A^2 \leq B^2 + C^2$ . Therefore:

$$X(t) \leq \mathcal{O}\left(\frac{1}{\tau^\sigma}\right) + 4B_\theta^2 Y(t) \quad (70)$$

For  $Y(t)$ , we have:

$$\begin{aligned} Y(t) &:= \frac{1}{(t - \tau + 1)} \sum_{k=\tau}^t \mathbb{E}[\|\boldsymbol{\omega}^* - \boldsymbol{\omega}_k\|^2] \\ &\leq \frac{2}{t} \sum_{k=\tau}^t \mathbb{E}[\|\boldsymbol{\omega}^* - \boldsymbol{\omega}_k\|^2] \end{aligned} \quad (71)$$

Finally, substitute the above inequalities into (62) yields:

$$\begin{aligned} \min_{\tau \leq k \leq t} \mathbb{E}[\|\nabla J(\boldsymbol{\theta}_k)\|^2] &\leq \frac{1}{t - \tau + 1} \sum_{k=\tau}^t \mathbb{E}[\|\nabla J(\boldsymbol{\theta}_k)\|^2] \\ &\leq \frac{B_\theta}{t - \tau + 1} 2B_\theta Y(t) + \frac{2c_\alpha R}{(1+\tau)^\sigma(t-\tau+1)} + \\ &\quad \frac{LB_j^2 c_\alpha}{2(1-\sigma)} \frac{1}{\tau^\sigma} + \epsilon_m + \frac{\epsilon_v^2}{4} \\ &= \mathcal{O}\left(\frac{\mathcal{E}(t)}{\tau}\right) + \mathcal{O}\left(\frac{1}{\tau^\sigma}\right) \end{aligned} \quad (72)$$

The proof is completed.  $\square$

## REFERENCES

- [1] H. Liu, T. Xue, and T. Schultz, "On a real real-time wearable human activity recognition system." in *HEALTHINF*, 2023, pp. 711–720.
- [2] P. Dini, G. Basso, S. Saponara, and C. Romano, "Real-time monitoring and ageing detection algorithm design with application on sic-based automotive power drive system," *IET Power Electronics*, 2024.
- [3] M. A. Abd-Elmagid, N. Pappas, and H. S. Dhillon, "On the role of age of information in the internet of things," *IEEE Communications Magazine*, vol. 57, no. 12, pp. 72–77, 2019.
- [4] P. Popovski, F. Chiariotti, K. Huang, A. E. Kalør, M. Kountouris, N. Pappas, and B. Soret, "A perspective on time toward wireless 6g," *Proceedings of the IEEE*, vol. 110, no. 8, pp. 1116–1146, 2022.
- [5] B. Quinn and K. Almeroth, "Ip multicast applications: Challenges and solutions," Tech. Rep., 2001.
- [6] S. Kaul, R. Yates, and M. Gruteser, "Real-time status: How often should one update?" in *2012 Proceedings IEEE INFOCOM*. IEEE, 2012, pp. 2731–2735.
- [7] R. D. Yates, Y. Sun, D. R. Brown, S. K. Kaul, E. Modiano, and S. Ulukus, "Age of information: An introduction and survey," *IEEE Journal on Selected Areas in Communications*, vol. 39, no. 5, pp. 1183–1210, 2021.
- [8] J. Li, Y. Zhou, and H. Chen, "Age of information for multicast transmission with fixed and random deadlines in iot systems," *IEEE Internet of Things Journal*, vol. 7, no. 9, pp. 8178–8191, 2020.
- [9] N. Pappas, M. A. Abd-Elmagid, B. Zhou, W. Saad, and H. S. Dhillon, *Age of Information: Foundations and Applications*. Cambridge University Press, 2022.
- [10] X. Jiang, F. R. Yu, T. Song, and V. C. Leung, "A survey on multi-access edge computing applied to video streaming: Some research issues and challenges," *IEEE Communications Surveys & Tutorials*, vol. 23, no. 2, pp. 871–903, 2021.
- [11] L. Yin, J. Gui, Z. Zeng *et al.*, "Improving energy efficiency of multi-media content dissemination by adaptive clustering and d2d multicast," *Mobile Information Systems*, vol. 2019, 2019.
- [12] C. A. Oliveira and P. M. Pardalos, "A survey of combinatorial optimization problems in multicast routing," *Computers & Operations Research*, vol. 32, no. 8, pp. 1953–1981, 2005.
- [13] J. Byrka, F. Grandoni, T. Rothvoß, and L. Sanita, "An improved lp-based approximation for steiner tree," in *Proceedings of the forty-second ACM symposium on Theory of computing*, 2010, pp. 583–592.
- [14] M. Fischetti, M. Leitner, I. Ljubić, M. Luipersbeck, M. Monaci, M. Resch, D. Salvagnin, and M. Sinnl, "Thinning out steiner trees: a node-based model for uniform edge costs," *Mathematical Programming Computation*, vol. 9, no. 2, pp. 203–229, 2017.

- [15] P. Paul and S. Raghavan, "Survey of multicast routing algorithms and protocols," in *Proceedings of the international conference on computer communication*, vol. 15, no. 3. Citeseer, 2002, p. 902.
- [16] D. Kreutz, F. M. Ramos, P. E. Verissimo, C. E. Rothenberg, S. Azodolmolky, and S. Uhlig, "Software-defined networking: A comprehensive survey," *Proceedings of the IEEE*, vol. 103, no. 1, pp. 14–76, 2014.
- [17] R. V. Ramakanth, V. Tripathi, and E. Modiano, "Monitoring correlated sources: Aoi-based scheduling is nearly optimal," *arXiv preprint arXiv:2312.16813*, 2023.
- [18] C. Pu, H. Yang, P. Wang, and C. Dong, "Aoi-bounded scheduling for industrial wireless sensor networks," *Electronics*, vol. 12, no. 6, p. 1499, 2023.
- [19] B. Fu, Y. Xiao, H. Deng, and H. Zeng, "A survey of cross-layer designs in wireless networks," *IEEE Communications Surveys & Tutorials*, vol. 16, no. 1, pp. 110–126, 2013.
- [20] L. Chen, S. H. Low, M. Chiang, and J. C. Doyle, "Cross-layer congestion control, routing and scheduling design in ad hoc wireless networks," in *Proceedings IEEE INFOCOM 2006. 25TH IEEE International Conference on Computer Communications*. IEEE, 2006, pp. 1–13.
- [21] M. S. Kuran, G. Gür, T. Tugcu, and F. Alagöz, "Cross-layer routing-scheduling in ieee 802.16 mesh networks," in *1st International ICST Conference on Mobile Wireless Middleware, Operating Systems and Applications*, 2010.
- [22] S. Cui, A. J. Goldsmith, and A. Bahai, "Energy-constrained modulation optimization," *IEEE transactions on wireless communications*, vol. 4, no. 5, pp. 2349–2360, 2005.
- [23] M. Xie, J. Gong, X. Jia, and X. Ma, "Age and energy tradeoff for multicast networks with short packet transmissions," *IEEE Transactions on Communications*, vol. 69, no. 9, pp. 6106–6119, 2021.
- [24] E. Khalil, H. Dai, Y. Zhang, B. Dilkina, and L. Song, "Learning combinatorial optimization algorithms over graphs," *Advances in neural information processing systems*, vol. 30, 2017.
- [25] Z. Wu, S. Pan, F. Chen, G. Long, C. Zhang, and S. Y. Philip, "A comprehensive survey on graph neural networks," *IEEE transactions on neural networks and learning systems*, vol. 32, no. 1, pp. 4–24, 2020.
- [26] P. Velickovic, G. Cucurull, A. Casanova, A. Romero, P. Lio, Y. Bengio et al., "Graph attention networks," *stat*, vol. 1050, no. 20, pp. 10–48 550, 2017.
- [27] G. Singal, V. Laxmi, M. S. Gaur, D. V. Rao, R. Kushwaha, D. Garg, and N. Kumar, "Qos-aware mesh-based multicast routing protocols in edge ad hoc networks: Concepts and challenges," *ACM Transactions on Internet Technology (TOIT)*, vol. 22, no. 1, pp. 1–27, 2021.
- [28] S. Kumar, A. Goswami, R. Gupta, S. P. Singh, and A. Lay-Ekuakille, "A game-theoretic approach for cost-effective multicast routing in the internet of things," *IEEE Internet of Things Journal*, vol. 9, no. 18, pp. 18 041–18 053, 2022.
- [29] D. Hatano and Y. Yoshida, "Computational aspects of the preference cores of supermodular two-scenario cooperative games," in *IJCAI*, 2018, pp. 310–316.
- [30] I. Ljubić, "Solving steiner trees: Recent advances, challenges, and perspectives," *Networks*, vol. 77, no. 2, pp. 177–204, 2021.
- [31] I. Kadota, A. Sinha, E. Uysal-Biyikoglu, R. Singh, and E. Modiano, "Scheduling policies for minimizing age of information in broadcast wireless networks," *IEEE/ACM Transactions on Networking*, vol. 26, no. 6, pp. 2637–2650, 2018.
- [32] J. Sun, L. Wang, Z. Jiang, S. Zhou, and Z. Niu, "Age-optimal scheduling for heterogeneous traffic with timely throughput constraints," *IEEE Journal on Selected Areas in Communications*, vol. 39, no. 5, pp. 1485–1498, 2021.
- [33] H. H. Yang, A. Arafat, T. Q. Quek, and H. V. Poor, "Optimizing information freshness in wireless networks: A stochastic geometry approach," *IEEE Transactions on Mobile Computing*, vol. 20, no. 6, pp. 2269–2280, 2020.
- [34] X. Chen, K. Gatsis, H. Hassani, and S. S. Bidokhti, "Age of information in random access channels," *IEEE Transactions on Information Theory*, vol. 68, no. 10, pp. 6548–6568, 2022.
- [35] R. D. Yates and S. K. Kaul, "The age of information: Real-time status updating by multiple sources," *IEEE Transactions on Information Theory*, vol. 65, no. 3, pp. 1807–1827, 2018.
- [36] A. M. Bedewy, Y. Sun, and N. B. Shroff, "Minimizing the age of information through queues," *IEEE Transactions on Information Theory*, vol. 65, no. 8, pp. 5215–5232, 2019.
- [37] L. Huang and E. Modiano, "Optimizing age-of-information in a multi-class queueing system," in *2015 IEEE international symposium on information theory (ISIT)*. IEEE, 2015, pp. 1681–1685.
- [38] B. Buyukates, A. Soysal, and S. Ulukus, "Age of information in multihop multicast networks," *Journal of Communications and Networks*, vol. 21, no. 3, pp. 256–267, 2019.
- [39] A. M. Bedewy, Y. Sun, and N. B. Shroff, "The age of information in multihop networks," *IEEE/ACM Transactions on Networking*, vol. 27, no. 3, pp. 1248–1257, 2019.
- [40] M. Sun, X. Xu, X. Qin, and P. Zhang, "Aoi-energy-aware uav-assisted data collection for iot networks: A deep reinforcement learning method," *IEEE Internet of Things Journal*, vol. 8, no. 24, pp. 17 275–17 289, 2021.
- [41] O. S. Oubbati, M. Atiquzzaman, H. Lim, A. Rachedi, and A. Lakas, "Synchronizing uav teams for timely data collection and energy transfer by deep reinforcement learning," *IEEE Transactions on Vehicular Technology*, vol. 71, no. 6, pp. 6682–6697, 2022.
- [42] E. Eldeeb, M. Shehab, and H. Alves, "Traffic learning and proactive uav trajectory planning for data uplink in markovian iot models," *IEEE Internet of Things Journal*, 2023.
- [43] F. Fu, X. Wei, Z. Zhang, L. T. Yang, L. Cai, J. Luo, Z. Zhang, and C. Wang, "Age of information minimization for uav-assisted internet of things networks: A safe actor-critic with policy distillation approach," *IEEE Transactions on Network Science and Engineering*, 2023.
- [44] X. Wu, X. Li, J. Li, P. Ching, and H. V. Poor, "Deep reinforcement learning for iot networks: Age of information and energy cost tradeoff," in *GLOBECOM 2020-2020 IEEE Global Communications Conference*. IEEE, 2020, pp. 1–6.
- [45] G. Bai, L. Qu, J. Liu, and D. Sun, "Aoi-aware joint scheduling and power allocation in intelligent transportation system: A deep reinforcement learning approach," *IEEE Transactions on Vehicular Technology*, 2023.
- [46] Q. Zhang and Y. Wang, "Correlated information scheduling in industrial internet of things based on multi-heterogeneous-agent-reinforcement-learning," *IEEE Transactions on Network Science and Engineering*, 2023.
- [47] X. He, C. You, and T. Q. Quek, "Age-based scheduling for mobile edge computing: A deep reinforcement learning approach," *IEEE Transactions on Mobile Computing*, 2024.
- [48] G. Stamatakis, N. Pappas, and A. Traganitis, "Control of status updates for energy harvesting devices that monitor processes with alarms," in *2019 IEEE Globecom Workshops (GC Wkshps)*. IEEE, 2019, pp. 1–6.
- [49] M. Hatami and M. Codreanu, "On the age-optimality of relax-then-truncate approach under partial battery knowledge in energy harvesting iot networks," in *2023 21st International Symposium on Modeling and Optimization in Mobile, Ad Hoc, and Wireless Networks (WiOpt)*. IEEE, 2023, pp. 589–596.
- [50] M. Xie, X. Jia, J. Yin, Q. Wang, and M. Zhou, "Age of information for partial earliest relay aided short packet status update with energy harvesting," *IEEE Transactions on Wireless Communications*, 2023.
- [51] M. Li, Y. Wang, and Q. Zhang, "Deep reinforcement learning for age and energy tradeoff in internet of things networks," in *2022 IEEE/CIC International Conference on Communications in China (ICCC)*. IEEE, 2022, pp. 1020–1025.
- [52] S. Nath, J. Wu, and J. Yang, "Optimum energy efficiency and age-of-information tradeoff in multicast scheduling," in *2018 IEEE International Conference on Communications (ICC)*. IEEE, 2018, pp. 1–6.
- [53] L. H. Sahasrabudde and B. Mukherjee, "Multicast routing algorithms and protocols: A tutorial," *IEEE network*, vol. 14, no. 1, pp. 90–102, 2000.
- [54] A. Sinha, L. Tassiulas, and E. Modiano, "Throughput-optimal broadcast in wireless networks with dynamic topology," in *Proceedings of the 17th ACM International Symposium on Mobile Ad Hoc Networking and Computing*, 2016, pp. 21–30.
- [55] M. Haenggi and D. Puccinelli, "Routing in ad hoc networks: a case for long hops," *IEEE Communications Magazine*, vol. 43, no. 10, pp. 93–101, 2005.
- [56] L. Bui, R. Srikant, and A. Stolyar, "Novel architectures and algorithms for delay reduction in back-pressure scheduling and routing," in *IEEE INFOCOM 2009*. IEEE, 2009, pp. 2936–2940.
- [57] D. Ogbe, C.-C. Wang, and D. J. Love, "On the optimal delay growth rate of multi-hop line networks: Asymptotically delay-optimal designs and the corresponding error exponents," *IEEE Transactions on Information Theory*, 2023.



- [58] M. C. Vuran and I. F. Akyildiz, "Error control in wireless sensor networks: a cross layer analysis," *IEEE/ACM transactions on Networking*, vol. 17, no. 4, pp. 1186–1199, 2009.
- [59] V. Asghari and S. Aissa, "Adaptive rate and power transmission in spectrum-sharing systems," *IEEE Transactions on Wireless Communications*, vol. 9, no. 10, pp. 3272–3280, 2010.
- [60] West and D. Brent, *Introduction to graph theory*. Prentice hall Upper Saddle River, 2001, vol. 2.
- [61] A. G. Barto and S. Mahadevan, "Recent advances in hierarchical reinforcement learning," *Discrete event dynamic systems*, vol. 13, pp. 341–379, 2003.
- [62] T. G. Dietterich, "Hierarchical reinforcement learning with the maxq value function decomposition," *Journal of artificial intelligence research*, vol. 13, pp. 227–303, 2000.
- [63] S. Brody, U. Alon, and E. Yahav, "How attentive are graph attention networks?" *arXiv preprint arXiv:2105.14491*, 2021.
- [64] Y. Zhang, G. Liao, S. Cao, N. Yang, N. Pappas, and M. Zhang, "Graph attention reinforcement learning for age-optimal multicast scheduling and routing," <https://github.com/Carlos0902/TGMS-Paper>, 2024.
- [65] P. Agarwal, M. Jleli, B. Samet, P. Agarwal, M. Jleli, and B. Samet, "Banach contraction principle and applications," *Fixed Point Theory in Metric Spaces: Recent Advances and Applications*, pp. 1–23, 2018.
- [66] V. Mnih, A. P. Badia, M. Mirza, A. Graves, T. Lillicrap, T. Harley, D. Silver, and K. Kavukcuoglu, "Asynchronous methods for deep reinforcement learning," in *International conference on machine learning*. PMLR, 2016, pp. 1928–1937.
- [67] R. S. Sutton, D. McAllester, S. Singh, and Y. Mansour, "Policy gradient methods for reinforcement learning with function approximation," *Advances in neural information processing systems*, vol. 12, 1999.
- [68] S. Mukherjee, F. Bronzino, S. Srinivasan, J. Chen, and D. Raychaudhuri, "Achieving scalable push multicast services using global name resolution," in *2016 IEEE Global Communications Conference (GLOBECOM)*. IEEE, 2016, pp. 1–6.
- [69] Q. Yu, H. Wan, X. Zhao, Y. Gao, and M. Gu, "Online scheduling for dynamic vm migration in multicast time-sensitive networks," *IEEE Transactions on Industrial Informatics*, vol. 16, no. 6, pp. 3778–3788, 2019.
- [70] J. Leskovec, J. Kleinberg, and C. Faloutsos, "Graphs over time: densification laws, shrinking diameters and possible explanations," in *Proceedings of the eleventh ACM SIGKDD international conference on Knowledge discovery in data mining*, 2005, pp. 177–187.
- [71] J. B. Kruskal, "On the shortest spanning subtree of a graph and the traveling salesman problem," *Proceedings of the American Mathematical society*, vol. 7, no. 1, pp. 48–50, 1956.
- [72] K. Zhang, A. Koppel, H. Zhu, and T. Basar, "Global convergence of policy gradient methods to (almost) locally optimal policies," *SIAM Journal on Control and Optimization*, vol. 58, no. 6, pp. 3586–3612, 2020.
- [73] Y. Nesterov *et al.*, *Lectures on convex optimization*. Springer, 2018, vol. 137.